

OPEN ACCESS

EDITED BY

Aglaia (cilia) Antoniou,
Hellenic Centre for Marine Research (HCMR),
Greece

REVIEWED BY

Daniele De Luca,
Suor Orsola Benincasa University, Italy
Son Le,
Vietnamese Academy of Forest Science,
Vietnam

*CORRESPONDENCE

Ludwig Triest

✉ ltriest@vub.be;

✉ Ludwig.Triest@ulb.be

[†]These authors have contributed equally to this work

RECEIVED 23 January 2025

ACCEPTED 17 April 2025

PUBLISHED 22 May 2025

CITATION

Triest L, Phan TTH, Luong QD,
Bousquet-Mélou A, Do BTN, Sierens T,
Dahdouh-Guebas F, Koedam N and Van der
Stocken T (2025) Migration history of
Avicennia marina populations: a legacy of
mangrove expansion on the Sunda Shelf.
Front. Mar. Sci. 12:1565908.
doi: 10.3389/fmars.2025.1565908

COPYRIGHT

© 2025 Triest, Phan, Luong, Bousquet-Mélou,
Do, Sierens, Dahdouh-Guebas, Koedam and
Van der Stocken. This is an open-access article
distributed under the terms of the [Creative Commons Attribution License \(CC BY\)](https://creativecommons.org/licenses/by/4.0/). The
use, distribution or reproduction in other
forums is permitted, provided the original
author(s) and the copyright owner(s) are
credited and that the original publication in
this journal is cited, in accordance with
accepted academic practice. No use,
distribution or reproduction is permitted
which does not comply with these terms.

Migration history of *Avicennia marina* populations: a legacy of mangrove expansion on the Sunda Shelf

Ludwig Triest^{1*†}, Thi Thuy Hang Phan², Quang Doc Luong²,
Anne Bousquet-Mélou³, Bich Thi Ngoc Do⁴, Tim Sierens⁴,
Farid Dahdouh-Guebas^{1,4,5}, Nico Koedam^{1,6,7}
and Tom Van der Stocken^{4†}

¹Systems Ecology and Resource Management Research Unit (SERM), Department of Organism Biology, Université Libre de Bruxelles (ULB), Brussels, Belgium, ²Biology Department, University of Sciences, Hue University, Hue, Vietnam, ³Institut Méditerranéen de Biodiversité et d'Ecologie marine et continentale (IMBE), Aix Marseille University, Avignon University, Centre national de la recherche scientifique (CNRS), French National Research Institute for Sustainable Development (IRD), Marseille, France, ⁴Ecology, Evolution and Genetics (bDIV) Research Group, Biology Department, Vrije Universiteit Brussel (VUB), Brussels, Belgium, ⁵Mangrove Specialist Group (MSG), Species Survival Commission (SSC), International Union for the Conservation of Nature (IUCN), Gland, Switzerland, ⁶Marine Biology Research Group, Universiteit Gent, Gent, Belgium, ⁷Centre for Environmental Sciences (CMK), Universiteit Hasselt, Diepenbeek, Belgium

Introduction: Mangrove forests maintain connectivity and stay genetically linked through ocean-dispersed propagules. *Avicennia* species exhibit a pronounced genetic structure following a stepping-stone migration model, with connectivity patterns linked to the strength and direction of ocean-surface currents. The present-day spatial genetic structure of *Avicennia marina* populations is an imprint of connectivity. This allows for estimating their migration history in relation to coastal configuration and Holocene sea-level rise.

Methods: We examined the genetic diversity, structure, and demographic and evolutionary history of the establishment of 10 *A. marina* sites across coastal stretches of Vietnam using nuclear microsatellite markers in 558 individual trees. Additionally, genome skimming of 24 samples allowed the detailed analysis of the complete chloroplast genome and nuclear ribosomal cistron sequences. Although *A. marina* grew mixed with *Avicennia alba*, a NewHybrids analysis ensured that only pure *A. marina* was considered in this study.

Results: Microsatellites revealed an overall low allelic diversity, although inbreeding, recent bottlenecks, and the strong differentiation of populations were detected. Genetic breaks along the coast were confirmed through AMOVA, structure, and barrier analyses, while $R_{ST} > F_{ST}$ indicated an evolutionary signal of divergence consistent with isolation by distance. MIGRATE-n model tests and DIVMIGRATE analysis supported northward unidirectional stepping-stone migration history. Approximate Bayesian computation (ABC) demographic analysis indicated a Holocene expansion, whereas an origin model demonstrated discrete migration events across Vietnam, with southern populations most closely related to a bottlenecked ancestral population. A haplotype network considering complete chloroplast genomes revealed identical or nearly similar propagule sources of *A. marina* throughout central

and northern Vietnam, thereby following the most recent Holocene expansion on the northwestern Sunda Shelf.

Discussion: Microsatellites, chloroplast, and rRNA cistron sequences confirmed the uniqueness of *A. marina* from the southernmost peninsula and their far relatedness with other populations in Southeast Asia, suggesting a longer-term persistence since gradual Shelf flooding. It is additionally proposed that, in addition to ocean currents, coastal landforms such as shallow areas with broad river delta plumes, a wide mouth, or strong discharge such as for the Mekong and Red Rivers may have caused a regional substructure and provided a quasi-permanent barrier to alongshore currents and mangrove connectivity. Perspectives on conservation issues of the species are provided.

KEYWORDS

Avicennia, genetic structure, connectivity, microsatellites, migration, dispersal, chloroplast genome, nuclear rRNA cistron

1 Introduction

Mangrove trees are adapted to grow in intertidal environments and occur along tropical, subtropical and some warm-temperate shorelines (Alongi, 2002). The degradation of remaining mangrove areas is a major concern, in both protected and unprotected areas (Goldberg et al., 2020; Heck et al., 2024), but receives less attention than terrestrial deforestation (Friess et al., 2019; Dahdouh-Guebas et al., 2022). Mangrove population persistence depends solely on the fruiting, release, distribution, and establishment of propagules, as any form of clonal growth or vegetative dispersal is absent in mangrove trees, except for the nipa palm. The connectivity of mangrove populations is determined by the spatial distribution of hydrochorous propagules and subsequent establishment and survival in suitable environments (Van der Stocken et al., 2019a). Viviparous mangroves produce propagules that lack a dormant stage and consist of seedlings, of which the dispersal success is contingent on reaching suitable establishment sites within their viability and buoyancy period (Rabinowitz, 1978; Van der Stocken et al., 2019a). Dispersal distances depend on the interaction between propagule and vector traits, environmental conditions such as landscape structure, biotic pressure such as from consumption by propagule predators (Dahdouh-Guebas et al., 2011), and factors such as fruiting phenology (Nathan et al., 2008). In mangroves, most propagules are dispersed within relatively short distances, but propagules reaching open waters can be transported over relatively long distances via river, tidal, longshore, and open-ocean currents (Clarke, 1993; Van der Stocken et al., 2015a; 2019a). Previous studies provided evidence for long-distance connectivity between mangrove populations, with connectivity patterns linked to the strength and direction of ocean-surface currents (Mori et al., 2015b; De Ryck et al., 2016; Ngeve et al., 2017; Hodel et al., 2018; Van der Stocken et al., 2019b) and the existence of mangrove patches, however small, as stepping stones for further

distribution (Curnick et al., 2019). This illustrates the importance of coastal population connectivity through gene flow. For mangrove species, this is nearly equivalent to propagule flow, as it is the only means of overseas dispersal between populations of discrete estuaries to maintain long-term evolutionary units.

However, barriers to genetic connectivity are posed by land masses and different migration histories (Triest, 2008; Hodel et al., 2018; Wee et al., 2020; Triest et al., 2021b), diverging ocean-surface currents (Mori et al., 2015a; Ngeve et al., 2016), or wide rivers with a strong discharge (Triest et al., 2018). In general, the expectation that dispersal routes follow major oceanic and coastal currents is largely confirmed with genetic markers when determining diversity and structure at the population level. A stepping-stone model of migration between coastal sites, based on isolation by distance has been reported regularly in *Avicennia* L. species (Maguire et al., 2000b; Do et al., 2019; Wee et al., 2020; Al-Qathanin and Alharbi, 2020; Triest et al., 2021a; e; Friis et al., 2024). Depending on the considered geographical range, a stepping-stone model was also found for *Rhizophora apiculata* Blume (Yan et al., 2016), *Sonneratia alba* J. Smith (Wee et al., 2020), *Lumnitzera littorea* (Jack) Voigt, *Lumnitzera racemosa* Willd (Guo et al., 2021; Manurung et al., 2023), and *Rhizophora stylosa* Griff. the latter between small islands (Thomas et al., 2022). Other case studies of mangrove species, such as *Rhizophora mucronata* Lam (Wee et al., 2014; Yan et al., 2016; Triest et al., 2021d), *R. stylosa* (Yan et al., 2016; Do et al., 2019), *Bruguiera gymnorrhiza* (L.) Lam. (Urashi et al., 2013; Wee et al., 2020), *S. alba* J. Smith (Wee et al., 2017), *L. racemosa* Willd (Li et al., 2016), *Xylocarpus granatum* J. Koenig (Tomizawa et al., 2017), and *Nypa fruticans* Wurmb (Mantiquilla et al., 2022), showed less clear isolation by distance (IBD) due to an overall low level of genetic diversity within and among populations over a large region.

Coastal ecosystems of the South China Sea (SCS)—also called the East Sea—are largely situated along a submerged rim of the

Sunda Shelf. In Southeast Asia, the Sunda Shelf forms large extensions of the Southeast Asian continental shelf and is characterized by shallow bathymetry (Hanebuth and Stattegger, 2004). Sea levels were estimated to have been approximately 116 m lower (Hanebuth et al., 2000) during the Last Glacial Maximum (LGM; 24–18 ka BP) than today (Mix et al., 2001). Progressive sea-level rise during subsequent deglaciation, into the early Holocene (from 11.7 ka BP onward), allowed mangroves to expand their range into suitable habitats along newly flooded shelf edges of the East Sea, from the Tonkin Gulf to the Gulf of Thailand, and toward the east and even west coast of the Malay Peninsula (Wee et al., 2014; 2015). Several studies have shown a pronounced land-barrier effect of the Malay Peninsula causing diverging ocean currents, resulting in genetically distinct mangrove populations on either side. This east–west genetic differentiation has been observed in multiple mangrove species, including *Avicennia alba* Blume, *Avicennia marina* (Forsk.) Vierh (Wee et al., 2020; Triest et al., 2021b), *B. gymnorhiza* (Minobe et al., 2010; Urashi et al., 2013; Wee et al., 2020), *Ceriops decandra* (Griff.) Ding Hou (Huang et al., 2008), *Ceriops tagal* (Perr.) C.B. Rob (Liao et al., 2007), *L. littorea* (Jack) Voigt (Su et al., 2007), *L. racemosa* (Su et al., 2006), *S. alba* (Yang et al., 2017; Wee et al., 2020), *Acanthus ilicifolius* Lam (Guo et al., 2020), *R. apiculata* (Inomata et al., 2009; Yahya et al., 2014; Ruang-areerate et al., 2022), *R. mucronata* (Wee et al., 2015, 2020), and other *Rhizophora* species (Yan et al., 2016). Considering differences in the dispersal capacity of several mangrove species, Wee et al. (2020) concluded that the Malay Peninsula acts as a filter for gene flow, rather than a strict barrier. Mixing of genotypes along the Malacca Strait as found in *X. granatum* (Tomizawa et al., 2017), *R. apiculata* (Azman et al., 2020), and *Aegiceras corniculatum* (L.) Blanco (Banerjee et al., 2022) may further support this hypothesis. Shallow land masses of the Sunda Shelf became ultimately flooded when reaching a maximum of +5-m sea level during the mid-Holocene at 4.2 ka BP (Sathiamurthy and Voris, 2006), hence allowing mangrove expansion beyond current shallow barriers. For *A. marina*, it was additionally proposed that colonization of the southwest coast of the Malay Peninsula could have occurred through migration from southern regions (Triest et al., 2021b).

Despite documented cases of strong genetic structure and distribution patterns in mangroves along the western part of the Sunda Shelf, less is known about the migration history of mangroves along the marginal northern Sunda Shelf edge, where a more than a 2,000-km coastal stretch allowed this coastal vegetation to establish progressively during the Holocene sea-level rise. These northern Sunda Shelf edge populations may remain genetically linked via recent dispersal events. Reported buoyancy periods are generally shorter for *Avicennia* than *Rhizophora* propagules (for an overview, see table 2 in Van der Stocken et al., 2019a), which may explain the strong genetic structure in *A. marina* as observed in comparison with *Rhizophora* over various distances in the northern part of Vietnam (Do et al., 2019). The present-day spatial genetic structure and variation of mangrove species along the entire coast of Vietnam still may reflect an imprint of their migration history following the change in the coastal configuration of the Sunda Shelf during post-LGM and Holocene sea-level rise.

There is ample prior knowledge on the application of sufficiently available polymorphic genetic markers for the geographically widespread gray mangrove *A. marina* and related species to achieve effective resolution at the estuary level and even at the individual level (Hermansen et al., 2015; Do et al., 2019; Al-Qthaini and Alharbi, 2020; Triest et al., 2020; Triest and Van der Stocken, 2021; Triest et al., 2021a; e; Lu et al., 2022). Some of the microsatellite loci of *Avicennia* species cross-amplify (Triest, 2008; Hasan et al., 2018; Triest et al., 2018; 2021a, b) or may show unique alleles at the taxon level so that instances of hybridization are detectable (Mori et al., 2015a; Triest et al., 2021b). Sequencing of maternal chloroplast DNA (cpDNA) introns or coding regions, and detecting polymorphism in nuclear ribosomal internal transcribed spacer (ITS) nowadays can be replaced by the shotgun method of next-generation sequencing (NGS) in high-throughput sequencing (HTS) technologies. Genome skimming offers time- and cost-effective production of large amounts of DNA data. Such shallow whole-genome sequencing targets the high copy regions of the genome, concerning the organellar genomes (i.e., the plastome and mitogenome) and the nuclear ribosomal cistron (Berger et al., 2017; Malé et al., 2014; Straub et al., 2012). The *de novo* assemblage of complete chloroplast genome sequences as well as concatenating the nuclear ribosomal RNA full cistron can be conducted at the individual level. The full cistron includes the three rRNA genes (18S, 5.8S, and 26S), their two internal transcribed spacers (ITS1 and ITS2), and more variable flanking regions with an external transcribed spacer (ETS) and a non-transcribed spacer (NTS) as presented by Linder et al. (2000). The combination of maternally inherited plastomes with the nuclear cistron can resolve phylogenomic questions at the species level, although potentially it can also address patterns of phylogeography at the population level, as shown for *R. mucronata* of the Western Indian Ocean (Triest et al., 2021c).

In this study, we focus on the connectivity pattern of *A. marina* populations along a 2,000-km-long coastline of Vietnam bordering the Sunda Shelf. We hypothesize that connectivity among regions would be pronounced among most recently established populations and that the directionality of historically accumulated gene flow would reflect dominant historical and contemporary ocean circulation patterns. We specifically aimed to 1) analyze the genetic diversity and structure of *A. marina* populations, 2) estimate the likelihood of stepping-stone migration models and their directionality between populations along the same coastline, and 3) estimate the ancestral and current population size with indication of divergence times of northern, central, and southern populations. To achieve this, we considered a combination of fast-evolving nuclear microsatellites, sequences of the nuclear ribosomal cistron, and maternally inherited complete chloroplast genomes. To estimate relationships and divergence times between *A. marina* populations of Vietnam and Southeast Asia, we compared microsatellite-based estimators of population structure with previous findings on *A. marina* from the Malay Peninsula (Triest et al., 2021b) and the Philippines (Triest et al., 2021a), and compared original sequences of the rRNA cistron and full plastome of samples from the latter regions with those of Vietnam.

2 Materials and methods

2.1 Plant materials

Fieldwork in Vietnam was conducted during 2013–2019, and a total of 558 individual trees were sampled (271 along the northern coast, 225 along the central region, and 62 along the southern coast) from 10 populations (Table 1; Figure 1A) over a maximum Euclidean distance of 1,430 km. Samples were collected using a transect approach for continuous patches and random sampling for discontinuous patches (the latter was practiced for S10 in Cà Mau Peninsula). Distances between neighboring trees were 2–5 m (occasionally 10 m) in the transects, whereas *A. marina* trees were scattered over ten to hundreds of meters in S10. Two mangrove populations of the southern region (S9 and S10) were not monospecific stands of *A. marina* but mixed with *A. alba* and could possibly contain hybrids. In those mixed populations, 171 adults and 73 juveniles of their putative species, in particular, were collected to verify the presence of hybrids in both generations. Leaves were collected into individually numbered paper envelopes, allowed to air or sun-dry until no moisture traces, and further preserved with silica gel for transportation and handling.

In order to estimate the relationship of the Vietnamese populations relative to other parts of Southeast Asia (see below), we additionally considered samples from outside the study area, namely, *A. marina* from Malaysia and the Philippines, as already published in Triest et al. (2021a, b), for a limited number of comparisons. These comprised 316 trees from three locations along a 275-km coastal stretch of western Peninsular Malaysia, namely, Penang Island (W1), Kuala Sepetang estuary in Matang, Perak (two transects: W2-A and W2-B), and Jeram in Kuala Selangor (W3); and 360 trees of six populations along the Western part of Leyte Island (115-km stretch), namely, Tabuk Islet in Palombon (AM5), Parilla in Palombon (AM6), Puertobello in Merida (AM9), Palhi in Baybay City (AM14),

Punta in Baybay City (AM15), and Esperanza in Inopacan (AM16) in the Philippines. We kept population codes as in Triest et al. (2021a, b).

2.2 DNA extraction and microsatellite genotyping

Genomic DNA was extracted from approximately 20 mg of each dried leaf tissue using the E.Z.N.A. SP plant DNA Mini kit (Omega Bio-tek, Norcross, GA, USA). The concentration of individual samples was measured on a NanoDrop One spectrophotometer (Thermo Fisher Scientific, Waltham, MA, USA) and ranged from 10 to 200 ng/μL. Fifteen microsatellite loci were amplified in one multiplex reaction and consisted of the following primers: Avma1, Avma02, Avma03, Avma05, Avma6, Avma8, Avma10, Avma14, and Avma17 (Geng et al., 2007); Am3 and Am81 (Maguire et al., 2000a); Aa22, Aa23, and Aa67 (Teixeira et al., 2003); and AMK6 (Triest et al., 2020). Primers were fluorescence-labelled with four different dye labels (6FAM, VIC, NED, and PET), and a mixture of 0.2 μM of each primer. Approximately 6.25 μL master mix (Qiagen Multiplex PCR kit, Hilden, Germany), 1.25 μL primer mix (2 μM of each primer), 2.5 μL H₂O, and 2.5 μL of genomic DNA were used for multiplex PCRs. PCR was performed in a thermal cycler (Bio-Rad MyCycler) under the conditions of initial denaturation at 95°C for 15 min followed by 35 cycles of 30-sec denaturation at 95°C, 90-sec annealing at 57°C, 80-sec elongation at 72°C, and a final extension of 30 min at 60°C. All PCR products were separated on an ABI3730XL sequencer (Applied Biosystems, Foster City, CA, USA) at MacroGen (Seoul, South Korea), and allele sizes were determined using GeneMarker v.2.60 (SoftGenetics LLC, State College, PA, USA).

A “comparative analysis” of Southern Vietnam populations with *A. marina* from Peninsular Malaysia (Southwest and West) and the Philippines (Leyte), as presented in Triest et al. (2021a, b),

TABLE 1 Location details of 10 *Avicennia marina* populations (14 transects) studied along the coast of Vietnam.

Code	Location	Province	North	East	Features
N1	Dong Rui–Tien Yen	Quang Ninh	21.24303	107.38828	Two transects
N2	Dai Hop–Kien Thuy Hai Phong	Hai Phong	20.69758	106.73466	One transect
N3	Thai Thuy	Thai Binh	20.51111	106.57914	One transect
N4	Xuan Thuy, Giao Xuan lagoon	Nam Dinh	20.22383	106.54631	Two transects
N5	Xuan Thuy, Giao Xuan lagoon	Nam Dinh	20.22155	106.48931	One transect
C6	Bu Lu river estuary	Thua Thien Hue	16.31389	107.97408	One transect
C7	Lap An	Thua Thien Hue	16.22636	108.08334	Two transects
C8	Tam Giang, Nui Thanh	Quang Nam	15.47319	108.65464	Two transects
S9	Thủy Triều lagoon	Khánh Hòa	12.04333	109.19559	Transect mixed with <i>Avicennia alba</i> .
S10	Cà Mau Peninsula	Cà Mau	8.638790	104.71598	Discontinuous, mixed with <i>A. alba</i>

Populations of *A. marina* were located in the northern (code N), central (code C), and southern (code S) regions.

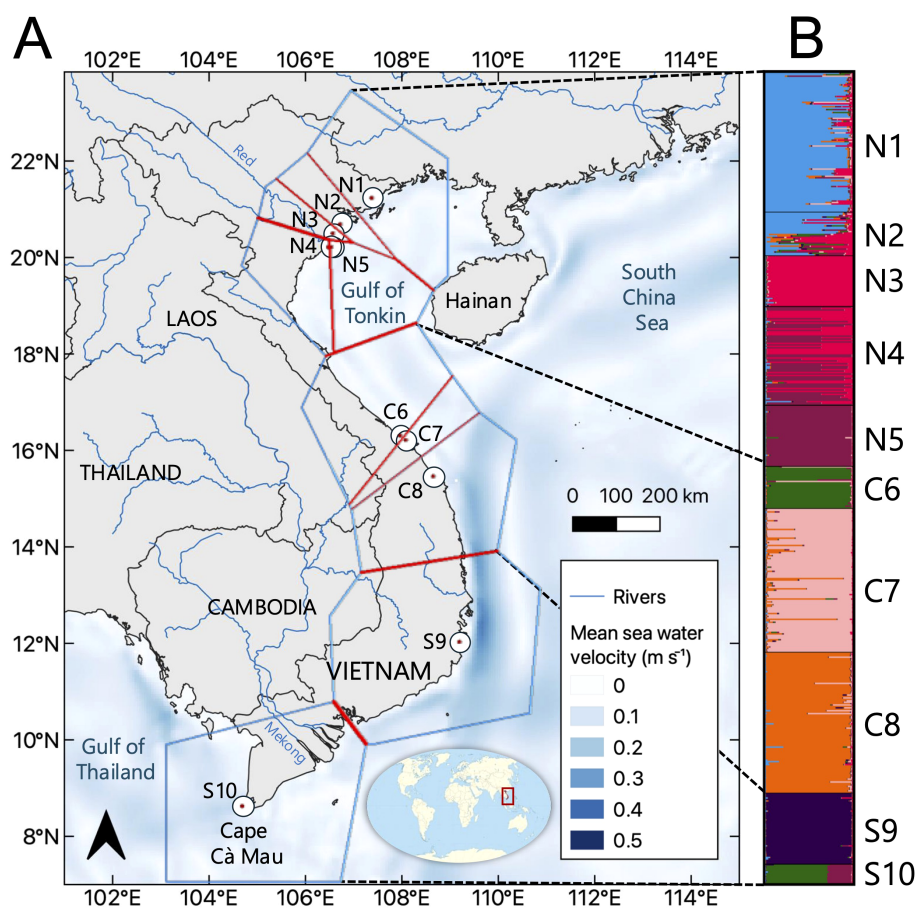


FIGURE 1

(A) Overview of the studied populations of *Avicennia marina* along the coast of Vietnam in the northern, central, and southern regions. Population codes are denoted as in Table 1, with polygons (blue lines) and genetic barriers (red lines) computed from F_{ST} distance matrices of independent microsatellite loci using BARRIER analysis. The thickness of the red line reflects the importance of the barriers. (B) STRUCTURE results of *A. marina* populations showing a strong substructure for $K = 7$ (see Supplementary Material). The background map was created with the QGIS 3.10.10 software (www.qgis.org) using country administrative boundaries, river center lines, and surface-water velocity data provided by Natural Earth (www.naturalearthdata.com).

was conducted for an overall available set of nine microsatellite loci (out of the abovementioned 15 loci)—Avma1, Avma02, Avma6, Avma8, Avma10, Avma14, Avma17, Am3, and Am81—and used only in a Principal Coordinate Analysis (PCoA) and for evolutionary model testing with ABC-RF (see further under microsatellite analysis). Locus Am3 was monomorphic in Leyte and, hence, was not retained in Triest et al. (2021a), although it could be considered in the current comparative study.

2.3 Complete chloroplast genome and rRNA cistron

For the analysis of the complete chloroplast genome and rRNA cistron, through genome skimming, 16 individuals covering all Vietnam sites (one in each transect from N1 to C8 and two in S9 and S10) were considered. For comparative reasons, seven individuals from the western coast of Leyte Island in the Philippines (one from each population AM5, AM6, AM8, AM9, AM14, AM15, and AM16 as

mentioned in Triest et al., 2021a) and three individuals from the western coast of Peninsular Malaysia (one from each population W1, W2, and W3 as mentioned in Triest et al., 2021b) were newly included and analyzed. Genomic DNA extracts of 26 samples were obtained at the Plant Biology and Nature Management (APNA) lab of the Vrije Universiteit Brussel (VUB) and processed for next-generation sequencing analysis using the E.Z.N.A. SP plant DNA Mini Kit (Omega Bio-tek, Norcross, GA, USA). Quantity and purity (260/280 and 260/230 ratios) of the DNA were determined using a NanoDrop One spectrophotometer (Thermo Fisher Scientific, Waltham, MA, USA). Extractions were repeated for samples with a 260/280 ratio of less than 1.8 and/or a concentration lower than 5 ng/ μ L. If necessary, multiple DNA extractions of the same individual were pooled and concentrated by ethanol precipitation. An Illumina paired-end library was constructed using the TruSeq Nano DNA Kit (Illumina, San Diego, CA, USA). After passing quality inspection (DNA concentration between 5 and 15 ng/ μ L), the constructed library was sequenced by 300 bp \times 2 paired-end sequencing (300PE) in an Illumina MiSeq platform (Macrogen, Seoul, South Korea).

2.4 Microsatellite data analysis

2.4.1 Hybrid detection of *A. marina* with *A. alba*

At first, there was a need to separate some of the *A. marina* trees from possible hybrids with sympatric *A. alba* of the two southern populations (S9 and S10), such that only pure *A. marina* individuals would be considered in this study. Pairwise genotypic differentiation of 244 individuals was used to produce a PCoA in GenAlEx v.6.5 (Peakall and Smouse, 2012) on a data set of the mixed southern Vietnam populations (S9 and S10) that included *A. marina* and *A. alba* adults and juveniles with the aim to remove all individuals with a potential hybridization signature. To evaluate the status of putative hybrid individuals and examine if there was backcrossing with one or both parents of each gene pool or if intercrossing happened among F_1 hybrid individuals (i.e., the production of F_2 or later generation), the method implemented in the NewHybrids 1.1 program was employed (Anderson and Thompson, 2002). This is a probability-based model, which computes through Markov chain Monte Carlo (MCMC) the posterior probability q_i of individuals belonging to distinct genealogical classes. Reference samples (reference parental genotypes) were *A. marina* and *A. alba*. The 244 individual unique genotypes were used and had no missing values. The following parameters were used: a burn-in period of 10,000 generations and 50,000 MCMC, Jeffrey's like priors, and the default six genealogical classes that correspond to i) pure *A. marina* gene pool [1.000/0.000/0.000/0.000], ii) pure *A. alba* gene pool [0.000/0.000/0.000/1.000], iii) F_1 hybrid [0.000/0.500/0.500/0.000], iv) F_2 hybrid [0.250/0.250/0.250/0.250], v) $B \times A. marina$ = backcross toward *A. marina* [0.500/0.250/0.250/0.000], and vi) $B \times A. alba$ = backcross toward *A. alba* [0.000/0.250/0.250/0.500]. This ensured that all further data analyses were performed solely on the genealogical class i) of pure *A. marina* individuals.

2.4.2 Population and individual sample-based analysis of pure *A. marina*

Prior to population and individual sample-based analysis of *A. marina* trees, data were tested for genotypic disequilibrium, potential null alleles, and overall resolution of the selected microsatellite markers. A linkage test between all pairs of loci (1,000 permutations) identified no genotypic disequilibrium at the 0.05 level (FSTAT v.2.9.3) (Goudet, 2001). MICRO-CHECKER indicated no scoring errors or large allele dropouts (Van Oosterhout et al., 2004). Null alleles were estimated using FreeNA (Chapuis and Estoup, 2007) and were not present throughout a particular locus or population, except for a few northern populations and those for two loci that were originally developed from *A. alba*. These potential null alleles with frequency > 0.3 were indicated for locus Aa23 in populations N3 and N4 and for locus Aa67 in populations N1 and N3, hence only in the northern region (Table 1; Figure 1A). FreeNA was used to adjust F_{ST} when correcting for null alleles. The probability of identity (PI), namely, whether two individuals could share an identical multilocus genotype by chance, was conducted using GenAlEx.

A population assignment test was carried out using the “leave-one-out” option, and frequencies of private alleles were obtained using GenAlEx. Basic population genetic variables were measured separately for each site and when pooled for the northern, central, and southern coastlines: total number of alleles (A_T), mean number of alleles (A_M), effective number of alleles (A_E), allelic richness (A_R) at $k = 13$ diploid individuals or 26 gene copies (i.e., the rarefied allelic richness for the smallest subsample of gene copies of constant size k , giving the expected number of alleles among k gene copies for comparison between populations), observed heterozygosity (H_O), unbiased expected heterozygosity (uH_E), and population inbreeding coefficient (F_{IS})—with 1,000 permutations test—using FSTAT and GenAlEx. To detect recent genetic bottlenecks in populations, Wilcoxon sign-rank tests were performed in the program BOTTLENECK (Piry et al., 1999), which are designed to identify expected heterozygosity excess at mutation–drift equilibrium (Luikart et al., 1998). The program was run on a two-phase mutation model (TPM) with a proportion in favor of the stepwise mutation model (70%). Pairwise genotypic differentiation at the individual level and pairwise F_{ST} at the population level were used to produce PCoAs in GenAlEx. The PCoA of individual trees was conducted for two data sets, namely, i) the full data set of *A. marina* in Vietnam and ii) a data set for comparison of *A. marina* populations of Vietnam with those of the Philippines (Triest et al., 2021a) and the Malay Peninsula (Triest et al., 2021b) to estimate a relative relationship of the Vietnam populations.

On the basis of co-dominant alleles (F -statistics) and microsatellite repeat lengths (R -statistics), the genetic structure among sites (F_{ST} and R_{ST}), inbreeding within sites (F_{IS} and R_{IS}), overall inbreeding (F_{IT} and R_{IT}), and a pairwise genotypic differentiation matrix (F_{ST}) of each species were calculated via AMOVA- F_{ST} and AMOVA R_{ST} at 999 random permutations (GenAlEx). A Mantel test was conducted using pairwise F_{ST} and Euclidean geographical distances of populations, considering 1,000 permutations. Euclidean distances could be used because their ranking is very similar to that of coastal distances. This allowed further testing for an evolutionary signal (when $R_{ST} > F_{ST}$) and to roughly estimate overall connectivity levels as $Nm = F_{ST}/(1 - 4F_{ST})$ under the assumption of an island migration model, an assumption that is very likely to be violated. Therefore, an alternative approach to investigate connectivity between populations was used; that is, a relative directional migration network was calculated using the DIVMIGRATE-online software (Sundqvist et al., 2016) based on the G_{ST} method for migration statistics and 1,000 bootstrap iterations for the statistical testing of the asymmetry between migration rates of all population pairs. A 0.25 threshold was used to show the most significant unidirectional migration rates. Furthermore, specific hypotheses to estimate gene flow between northern, central, and southern Vietnam regions were tested using MIGRATE-n (Beerli, 2006; Beerli and Palczewski, 2010) from the mutation-scaled population sizes (Θ) and immigration rates (M). The Brownian model was tested locus by locus along with the product of all distributions of all loci. Uniform prior distribution settings (min, max, delta) were as follows: $\Theta = 0.0, 20.0, 2$ and $M = 0.0, 20, 2$. The number of

recorded steps was 10^6 at a sampling frequency of 10^3 after an initial burn-in. The effective number of immigrants per generation ($N_e m$) was calculated as $[\Theta \times M]/4$. Specific hypothesis testing on directionality was considered in panmixia (full model), bidirectional, and unidirectional stepping-stone models for the migration of mangroves between three regions situated along the same coastline. More precisely, all 10 *A. marina* populations of the three regions were considered to test the hypothesis of a northward (historically prevailing), southward, or bidirectional coastal current direction in this part of the South China Sea. The Brownian motion mutation model was adopted for randomly generated subsamples of 20 individuals in a transect, following the abovementioned settings, computing two replicate chains (with different seeds), and using the Bezier thermodynamic integration (Beerli and Palczewski, 2010) for the calculation of the Bayes factors from marginal likelihoods giving the model probabilities.

A Bayesian clustering analysis at the individual level for 10 *A. marina* populations was carried out with STRUCTURE v.2.3.4 (Pritchard et al., 2000) using an admixture model with correlated allele frequencies. The model ran 10 iterations for each K value from 1 to 12; the burn-in period was 50,000 with 500,000 MCMC repeats. Analyses were computed after downloading the data on the Galaxy web platform using the public server at UseGalaxy.be (The Galaxy Community, 2022). The optimal K was inferred with the ΔK statistic (Evanno et al., 2005), $\text{LnP}(K)$, and the MedK estimator (Puechmaillie, 2016) using Structure Harvester (Earl and von Holdt, 2012) calculated with StructureSelector (Li and Liu, 2018). In addition, barplots were built for each K using the CLUMPAK option in StructureSelector, and the highest values for the “divisions of run by mode” provided by CLUMPAK were considered alternative estimators at various thresholds in addition to ΔK , together with a visual inspection of gene pools and Q values of assignments, because the ΔK method may show downward bias in its estimation of K and is sensitive to uneven sampling (Stankiewicz et al., 2022). The genetic cluster $K = 2$ (following a STRUCTURE outcome) was considered for the calculation of standard genetic diversity measures A_E , H_O , H_E , and AMOVA- F_{ST} . The BARRIER v.2.2 software (Manni et al., 2004) was used to additionally detect the location of sharp genetic changes between neighboring populations on the basis of 15 pairwise F_{ST} matrices of every microsatellite locus, allowing a maximum of one barrier per matrix. We opted to calculate from the superposition of raw data from F_{ST} matrices at the locus level. The thickness of barrier lines will thus be based on the additivity of matrices accounting for the independent microsatellite loci that we consider a preferred informative and valid method over bootstrapping a single mean F_{ST} matrix (Triest et al., 2020).

We based the demographic history of divergence between *A. marina* populations of northern, central, and southern Vietnam on respective pooled samples of microsatellites using the approximate Bayesian computation (ABC) approach implemented in DIYABC-Random Forest v1.0 (Collin et al., 2021). We narrowed down the ABC scenario testing with subsequent demographic models at the species level (here abbreviated as ABC1: Supplementary Figure S1) and origin models for three regions (northern, central, and southern)

at the Vietnam level (abbreviated ABC2: Supplementary Figure S1). We first tested for overall demographic events (ABC1 = demographic model with 4 scenarios): 1) constant population size, 2) population decline, 3) population expansion, and 4) population bottleneck followed by an expansion. For the Vietnamese *A. marina*, we used all 10 *A. marina* provenances considered one pooled sample to conduct these conceptualized scenarios of demographic history. We considered summary statistics of 12 variables, including five noise variables as default. For this demographic model (ABC1) at species level restricted to the Vietnam coastline, we used a training set of 40,000 runs and broad time priors (10–10,000) for t_1 , t_0 , and duration of bottleneck $db (= t_0 + dt)$ and broad effective size priors on N_e , N_{de} (decline), N_{ex} (expansion), and N_{e1} (10–10,000), although restricted sizes for the bottleneck N_{bo} (10–2,500).

Analyses of origin models (ABC2) of northern (N1), central (N2), and southern (N3) populations, considering all seven possible combinations as scenarios (Supplementary Figure S2), were performed to answer the main phylogeographic questions of expansion (i.e., based on the outcome of ABC1). Questions were equally raised from the phylogenetic outcome (an evolutionary signal from R_{ST} when higher than F_{ST}) and the geographical distribution and clusters of gene pools. The following were therefore tested: 1) a potential ancestral origin of the southern Vietnam populations (“Sunda remnant” hypothesis) and 2) the origin and (generation) time of expansion of central and northern Vietnam populations. A training set of 70,000 runs and time priors for t_1 and td (10–10,000) with effective size priors on N_{eA} , N_{e1} , N_{e2} , and N_{e3} (all 10–10,000) were used. The timing of inferred demographic events then could be estimated from the computed posterior distribution of time parameters from the best model choice (% votes and probability out of 500 runs). In all scenarios, $t\#$ represents the time scale measured in number of generations (largest numbers refer to oldest events), and $N\#$ represents the effective size of the corresponding populations during the indicated time period. Default prior values for all parameters were used. Summary statistics of 50 variables including five noise variables were considered for each population or pairwise comparison of three samples: one-sample summary statistics were genetic diversities, and two-sample summary statistics were F_{ST} distances and Nei’s distances, all considering the proportion of zero values, mean of non-zero values, variance of non-zero values, and mean of the complete distribution. The most likely scenario was obtained from a comparative assessment of their posterior probabilities. The goodness-of-fit was checked through principal component analysis (PCA) using the “out of bag” error method as implemented in DIYABC-RF (Collin et al., 2021). The posterior distribution of parameters ($N\#$ and $t\#$) was estimated for each of the most likely supported scenarios. The generation time of *Avicennia*, i.e., the average interval between the formation of an individual propagule and the production of its offspring, is minimal $t = 3$ years when under stress (Stuart et al., 2007) although usually $t = 5$ years (J. Kairo, pers. obs.). Additionally, the distance between individuals of one generation and the next is highly influenced by overlapping generations, namely, when offspring will, after maturation, also have their own cohort of propagules,

simultaneously with the parent generation that could be breeding again as well. Considering the minimum time span and overlapping generations, we propose here to use $t = 3$ to 5 when converting generations into years.

2.5 Chloroplast genome assembly, alignment, and comparative analysis

Raw data were filtered out to remove the joint sequence and low-quality reads to obtain high-quality clean data. The Illumina paired-end reads were used for genome skimming of *de novo* chloroplast assemblies. A *de novo* chloroplast assembly was conducted at first from a fresh and good-quality specimen of *A. marina* from Kenya (Gazi Bay) using NOVOPlasty assembly at Kmer = 33 and developed by Dierckxsens et al. (2017). The Illumina paired-end reads were used for chloroplast assemblies that were referenced to the existing annotated *A. marina* chloroplast genome (GenBank accession number MT108381 from Fujian, China, by Li et al., 2020) and the assemblies that appeared similar in genome structure and perfectly aligned with our reference sample from Kenya (as used by Dierckxsens et al., 2017) although did not align well with GenBank accession number MT012822 (*A. marina* from Oman by Khan et al. in 2020, unpublished). All 26 individual samples (16 from Vietnam, 7 from the Philippines, and 3 from Malaysia) were assembled using the “assemble to reference” function in the Geneious software. Illumina 2 × 300 bp paired-end was processed in Geneious Prime® 2024.0.5 (Biomatters Ltd., Auckland, New Zealand) to obtain complete chloroplast genome sequences. This approach facilitated the analysis without the need to describe *de novo* chloroplast genome features and gene annotations. The 26 consensus complete chloroplast sequences were aligned with MAFFT v7.388 (Katoh and Standley, 2013). Manually adjustments were conducted at sites with mononucleotide repeats and insertions/deletions (indels). All mutational steps were considered for manual haplotype definition on the basis of transitions, transversions, indels, and mononucleotide repeats. Indels were considered a single event regardless of their size and recoded as proposed by Müller (2006). A minimum spanning network using NETWORK 10.1 (Fluxus Engineering) served as a haplotype definition on the basis of 128 mutational characters. In this paper, the term “haplogroups” was used for the three major clusters A, B, and C, and their minor variants were designated as “haplotypes”.

2.6 Nuclear rRNA cistron assembly

Genome skimming allowed for assembling the nuclear ribosomal cistron (18S, ITS1, 5.8S, ITS2, and 26S) from a 671-bp template sequence of *A. marina* (Genbank AF365978, Schwarzbach and McDade, 2002) containing an internal transcribed spacer 1 (partial sequence), 5.8S ribosomal RNA gene (complete sequence), and internal transcribed spacer 2 (partial sequence) and subsequently used four times as a seed in Geneious Prime®

2024.0.5 to progressively enlarge the flanking regions. The generated consensus sequences of 5,772-bp length for a total of 26 samples (16 from Vietnam, 7 from the Philippines, and 3 from Malaysia) were aligned for the comparative description of mutated positions using MAFFT v7.388 (Katoh and Standley, 2013).

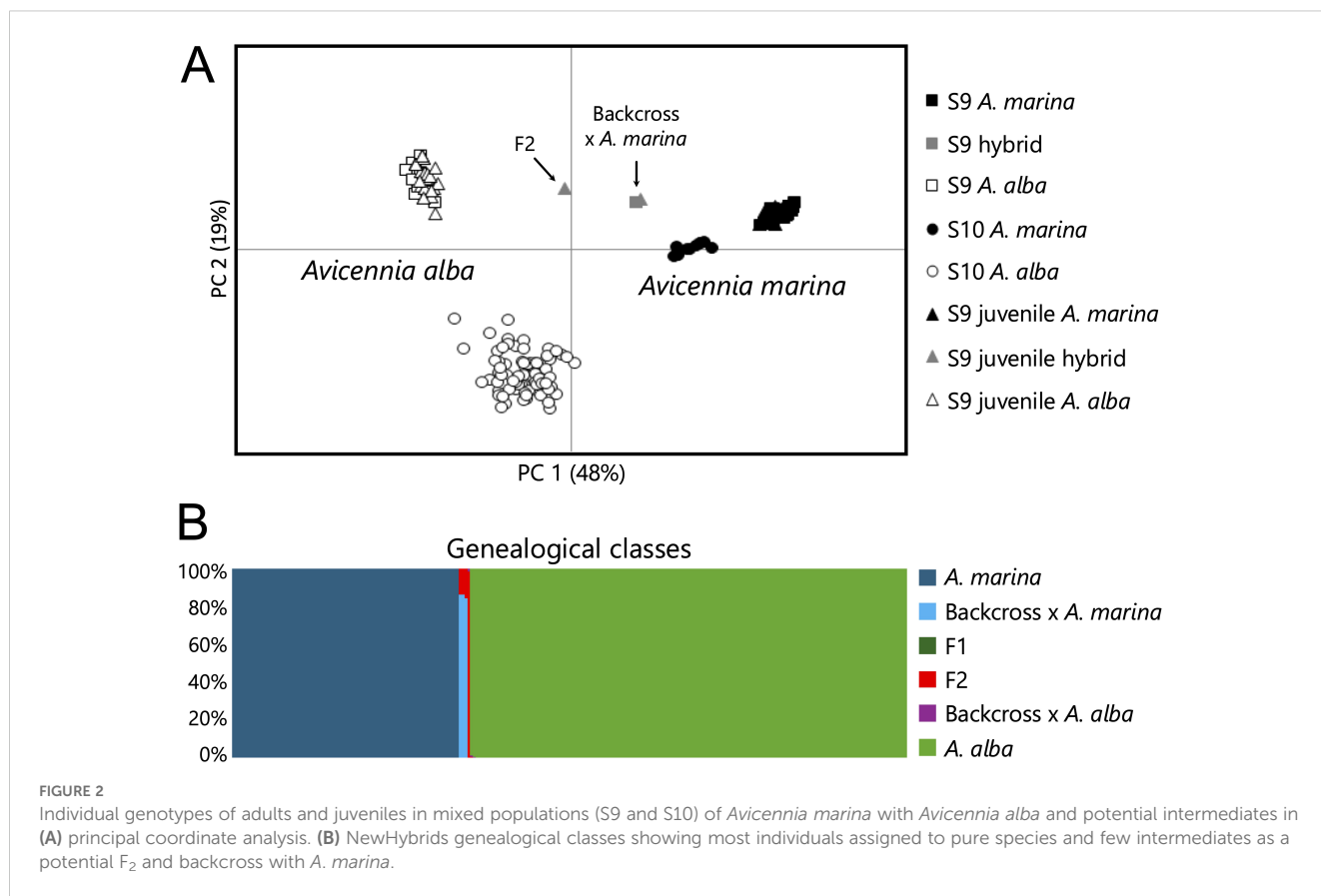
3 Results

3.1 Hybrid detection

The southern populations of *A. marina* co-occurred with *A. alba*; hence, it was necessary prior to in-depth data analysis to remove all genotyped individuals carrying a potential influence of hybridization with *A. alba*. Nuclear microsatellite markers confirmed three disjunct gene pools in mixed population S9. In S9, both adult trees and seedlings of “pure” *A. marina* and “pure” *A. alba* were present, as well as a few second-generation (F_2) or backcrossed adults and seedlings. Despite mixed patches of both species in S10, only two clearly distinct gene pools referring to each species were detected. A PCoA of all individuals from two mixed populations revealed a clear separation of the *A. marina* trees, *A. alba* trees, and a few intermediates that may represent hybrids in population S9, although not in southernmost population S10 (Figure 2A). The NewHybrids analysis (Figure 2B) showed that out of 244 unique genotypes, 82 individuals were undoubtedly classified as a pure gene pool of *A. marina* (Q between 0.999 and 0.998) and 158 individuals as a pure gene pool of *A. alba* (Q between 0.991 and 1.0). A single juvenile individual of population S9 was clearly assigned as an F_2 hybrid (Q = 0.98), whereas none could be assigned as F_1 . Only three individuals from population S9 were classified as potential backcrosses with *A. marina* (Q = 0.84–0.86 for one juvenile and two adult individuals). No backcrosses with *A. alba* were suggested. Both populations S9 and S10 thus contained a majority of individuals that were assigned to a single gene pool of either species. Hence, only the adult trees of populations S9 and S10 that were assigned to *A. marina* have been considered for all further genetic diversity analyses described hereafter. Moreover, all remaining and putative “pure” *A. marina* individuals were genotypically checked for possible introgression of alleles coming from *A. alba*. This could be verified with certainty since diagnostic *A. alba* alleles were documented. Any further introgressive hybridization through backcrossing could not be evidenced such that the individuals of southern populations indeed only featured *A. marina* allelic variation.

3.2 Genetic diversity of nuclear microsatellites in *A. marina*

The probability of identity (PI), namely, whether two individuals could share an identical multilocus genotype by chance, gave a cumulative probability of identity for all polymorphic microsatellite loci and ranged per site from 9.4×10^{-8} to 1.1×10^{-3} (except population N5 with 1.2×10^{-2}), thereby



providing ample resolution. A total of 95 alleles (on average 34 and ranging from 20 to 54 per population) were detected in 15 microsatellite loci from 10 sampling sites along the coast of Vietnam, with a mean (A_M) number of 1.3–3.6, effective (A_E) number of 1.1–2.2 and an adjusted richness (A_R) of 1.2–2.8 (Table 2). The overall observed heterozygosity ($H_O = 0.147$) was lower than the unbiased expected heterozygosity ($uH_E = 0.230$). The within-population inbreeding F_{IS} ranged from 0.165 to 0.786 and was significant ($p < 0.05$) for nine sites (Table 2). A population assignment test assigned as much as 98% of the individual trees to their own population and in particular for all individuals of S10. Populations N1 to N5 from the northern region showed eight private (= unique) alleles (at an average frequency of $\hat{q} = 0.021$), central populations had eight private alleles ($\hat{q} = 0.048$), and southern populations S9 and S10 were distinguished with 24 private alleles and at higher frequencies of $\hat{q} = 0.209$ (Supplementary Table S1). A significant excess of heterozygotes ($p < 0.05$) at mutation–drift equilibrium was detected in a BOTTLENECK test of each population, which may suggest that all locations have experienced recent bottlenecks in effective population size.

AMOVA- F_{ST} results revealed 46% genetic variation among *A. marina* populations, 21% among individuals, and 33% within individuals, giving estimates of $F_{ST} = 0.462$, $F_{IS} = 0.385$, and $F_{IT} = 0.669$ (Table 3). When adjusting for null alleles, $F_{ST} = 0.447$. AMOVA- R_{ST} gave higher estimates of genetic variance among the populations than F_{ST} with $R_{ST} = 0.598$ (60%); hence, this

larger differentiation indicated an evolutionary signal due to allele repeat length of the microsatellites (mutational steps) rather than of allele identity only (Table 3). Considering a hierarchy of three regions, the AMOVA- F_{RT} revealed 23% genetic variation among the northern, central, and southern regions, whereas another 27% among populations have an estimate of $F_{RT} = 0.230$, $F_{SR} = 0.353$, and $F_{ST} = 0.502$ (Table 3). AMOVA- R_{ST} gave higher estimates of genetic variance among the regions and the populations than F_{ST} with $R_{RT} = 0.242$, $R_{SR} = 0.511$, and $R_{ST} = 0.630$ (Table 3). All AMOVA- F_{ST} -based gene flow estimates were lower than $Nm = 0.3$.

The pairwise genetic differentiation of the nuclear microsatellites was the highest for populations between the three regions ($F_{ST} = 0.272$ – 0.773), whereas differences between locations of the same region could be more distinct for northern sites ($F_{ST} = 0.147$ – 0.677) and southern sites ($F_{ST} = 0.627$) than for those of the central region ($F_{ST} = 0.218$ – 0.422) (Supplementary Table S2). This F_{ST} approach indicates an overall poor connectivity among the *A. marina* populations and the considered regions. A Mantel test showed an overall isolation by distance of pairwise F_{ST} values over 1,430 km ($y = 0.0002x + 0.4$; $r = 0.5$ with $p = 0.003$). The PCoA of individual genotypes (Figure 3A) separated most of the individuals from northern sites from the ones from central sites along a first axis (22% explained) without further geographical gradient. A southern population (S9) fully separated along a second axis (14% explained). All individual trees from the southernmost population (Cà Mau Peninsula—S10) could be clearly separated along the third (10%) and fourth (8%) axes. The sample

TABLE 2 Population genetic variables of *Avicennia marina* populations in mangrove areas along the Vietnam coastline.

Site	N	A_T	A_M	A_E	A_R	H_O	uH_E	F_{IS}	cpDNA haplotype	rRNA cistron
N1	96	54	3.6 ± 0.5	2.2 ± 0.3	2.8	0.278 ± 0.046	0.435 ± 0.070	0.368*	Aa	A
N2	30	37	2.5 ± 0.5	1.9 ± 0.3	2.3	0.200 ± 0.066	0.290 ± 0.078	0.325*	Ab	A
N3	35	24	1.6 ± 0.2	1.3 ± 0.1	1.4	0.116 ± 0.064	0.167 ± 0.062	0.318*	Ac	A
N4	68	25	1.7 ± 0.2	1.4 ± 0.2	1.5	0.046 ± 0.020	0.174 ± 0.065	0.739*	Ad	A
N5	42	20	1.3 ± 0.1	1.1 ± 0.1	1.2	0.016 ± 0.007	0.073 ± 0.045	0.786*	Ac	A
C6	29	29	1.9 ± 0.3	1.4 ± 0.2	1.8	0.156 ± 0.057	0.183 ± 0.063	0.165	Ae	A
C7	99	37	2.5 ± 0.5	1.5 ± 0.3	2.1	0.105 ± 0.038	0.213 ± 0.067	0.511*	Ae	A
C8	97	40	2.7 ± 0.5	1.6 ± 0.2	2.1	0.187 ± 0.055	0.243 ± 0.071	0.236*	Af	A
S9	49	50	3.3 ± 0.4	1.7 ± 0.2	2.7	0.227 ± 0.054	0.305 ± 0.069	0.265*	Ae, Ag	A
S10	13	28	1.9 ± 0.2	1.4 ± 0.1	1.9	0.138 ± 0.043	0.216 ± 0.055	0.392*	Ah, Ai	A°
Total	558	95								
Mean	55.8	34.4	2.3 ± 0.1	1.4 ± 0.1	2.0	0.147 ± 0.016	0.230 ± 0.021			

* F_{IS} at $p < 0.05$ significance level.

N, number of genotyped samples; A_T , total number of alleles; A_M , mean number of alleles; A_E , effective number of alleles; A_R , allelic richness adjusted for 13 diploid individuals; H_O , observed heterozygosity; uH_E , unbiased expected heterozygosity; F_{IS} , within-population inbreeding; cpDNA haplotype, identity on the basis of complete chloroplast genome; rRNA cistron, identity on the basis of three nuclear ribosomal genes including spacers ITS1 and ITS2 and flanking regions with (°) indicating an incomplete homogenization.

eigenvectors of axis 4 ranged from 0.42 to 0.61 for 13 individuals from S10, while for all other 545 individuals from different Vietnamese locations, they ranged from -0.28 to 0.38. The identity of *A. marina* individuals of southern Vietnam was further compared with that of *A. marina* from Southeast Asia in a PCoA and showed a clear gradient and grouping of individuals along a first axis (22%) from the Malay Peninsula, the Philippines, and southern Vietnam (S9 and S10) and along a second axis (21%) in both central and northern Vietnam (Figure 3B). A population-based PCoA separated the populations of a central and northern group and additionally separated two southern populations. The first axis explained 28%, and the second axis explained 22% of the variation (Supplementary Figure S3).

3.3 Genetic structure, coastal connectivity, and gene flow models of *A. marina*

The BARRIER analysis showed several genetic breaks, the strongest between two southern populations (S9 and S10), between southern (S9) and central populations (C8), and also for N3 (Figure 1A). The Bayesian clustering analysis of 558 *A. marina* samples indicated well-separated gene pools and assigned many individuals to a single gene pool with limited admixture (Figure 1B). Delta K was high for $K = 2$ and $K = 7$. The latter outcome of $K = 7$ was supported by each iteration (giving a low standard deviation) and approached the $\ln P(K)$ plateau and the alternative MedK method with eight clusters (Supplementary Figure S4). Seven populations (N1, N3, N5, C6, C7, C8, and S9) were homogenous and represented their own gene pool. Northern site N2 shared assignments of N1 and N3, whereas N4 shared assignments with the nearby N5. All S10 individuals appeared mixed at $K > 2$ cluster

levels. When considering the genetic cluster $K = 2$ (i.e., the northern and southern populations combined versus the central populations) instead of 10 predefined sampled population sites, the genetic diversity measures showed lower diversity levels for the central region ($A_E = 1.8$; $H_O = 0.15$; $H_E = 0.28$) than for the combined northern plus southern cluster ($A_E = 2.2$; $H_O = 0.16$; $H_E = 0.44$). Both clusters at $K = 2$ were differentiated with an AMOVA- $F_{ST} = 0.260$ ($p < 0.001$).

The relative directional migration network (DIVMIGRATE) of 10 populations showed only significant connectivity within the northern region (Table 4; Supplementary Figure S5) where population N5 featured as a source population with unidirectional migration rates toward populations N1, N2, and N4 that all appear to be involved in a northern network. Population N3 at somewhat different geographic positions (i.e., close to a Red River branch in an enclosed delta and located on the landward side) showed no connectivity. Specific testing with MIGRATE-n on the directionality for *A. marina* across three regions of the Vietnamese coast indicated that panmixia, bidirectional stepping-stone models (from south to north as well as from north to south), and unidirectional north to south migration are less likely than a unidirectional south to north migration (Table 4). The highest estimated gene flow values were observed from the central region toward the northern region ($N_e m = 2.9$) when compared to movement from the southern region toward the central region ($N_e m = 1.3$). These were concordant with the genetic break evidenced by the BARRIER (Figure 1A) and STRUCTURE analyses (Figure 1B).

The demographic analysis (ABC1) for the whole Vietnamese coastline setting (10 populations as a single pool) showed support (46% votes; post probability 0.52) for scenario 3 referring to an overall expansion history of the species (Figure 4A). The median expansion event was estimated at $t_1 = 4,816$ with a large and

TABLE 3 Summary of AMOVA with *F*-statistics and *R*-statistics of *Avicennia marina* mangrove populations along coastline of Vietnam.

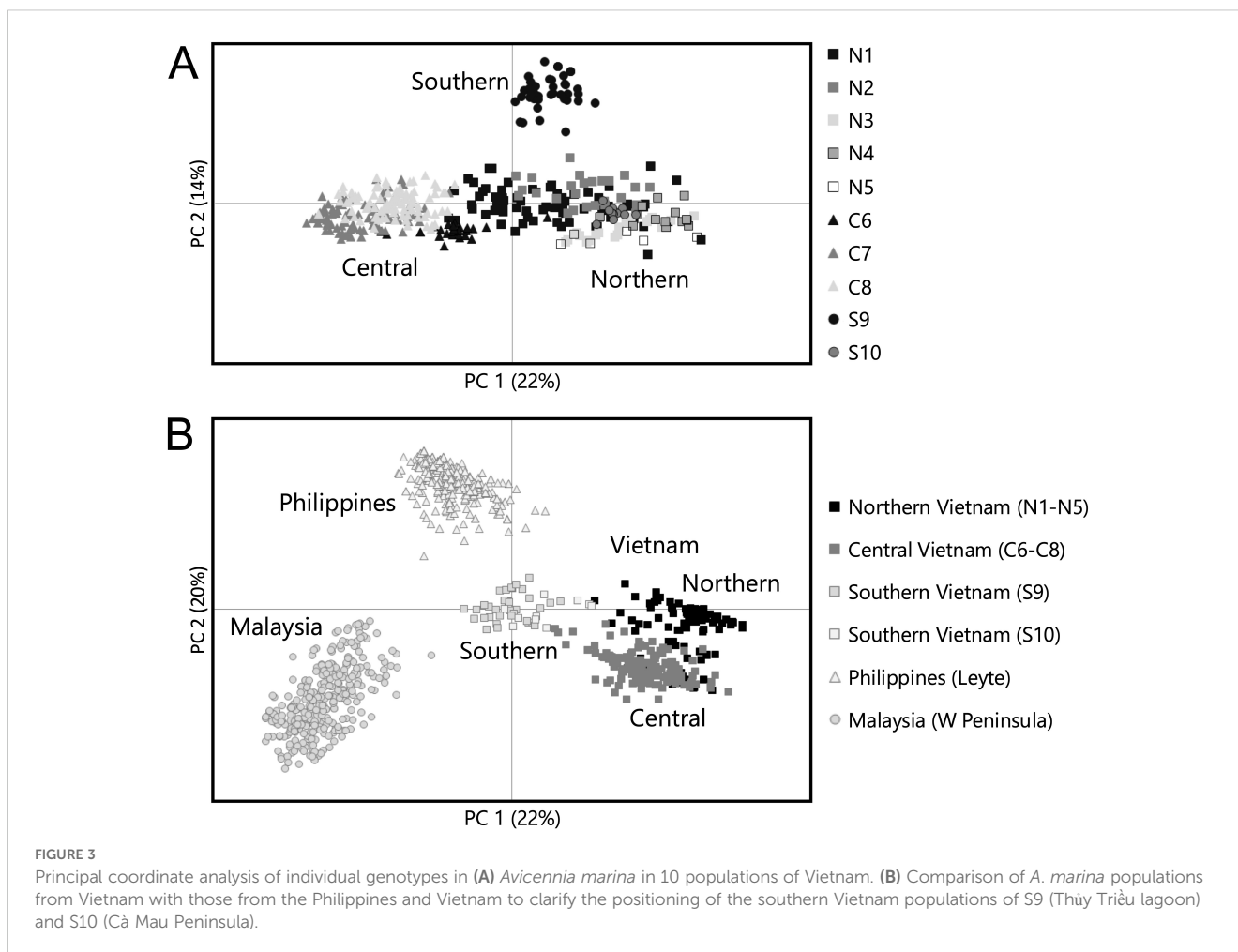
	df	SS	MS	Est. Var.	%	F-statistics	p-Value
<i>A. marina</i> (population level)							
Among pops	9	1599,162	177,685	1,622	46%	$F_{ST} = 0.462$	0.001
Among individual	548	1435,951	2,620	0,729	21%	$F_{IS} = 0.385$	0.001
Within individual	558	649,000	1,163	1,163	33%	$F_{IT} = 0.669$	0.001
Total	1,115	3684,113		3,514	100%	$Nm = 0.29$	
Among pops	9	82169,515	9129,946	83,907	60%	$R_{ST} = 0.598$	0.001
Among individual	548	40448,232	73,811	17,479	12%	$R_{IS} = 0.310$	0.986
Within individual	558	21679,500	38,852	38,852	28%	$R_{IT} = 0.723$	0.001
Total	1,115	144297,247		140,238	100%	$Nm = 0.17$	
<i>A. marina</i> (hierarchy of 3 regions)							
Among regions	2	833,504	416,752	0,871	23%	$F_{RT} = 0.230$	0.001
Among pops	7	765,658	109,380	1,032	27%	$F_{SR} = 0.353$	0.001
Among individual	548	1435,951	2,620	0,729	19%	$F_{ST} = 0.502$	0.001
Within individual	558	649,000	1,163	1,163	31%	$F_{IS} = 0.385$	0.001
Total	1,115	3684,113		3,795	100%	$F_{IT} = 0.694$	0.001
						$Nm = 0.25$	
Among regions	2	38978,738	19489,369	36,884	24%	$R_{RT} = 0.242$	0.001
Among pops	7	43188,351	6169,764	58,937	39%	$R_{SR} = 0.511$	0.001
Among individual	548	40448,587	73,811	17,481	11%	$R_{ST} = 0.630$	0.001
Within individual	558	21677,500	38,849	38,849	26%	$R_{IS} = 0.310$	0.001
Total	1115	144293,176		152,151	100%	$R_{IT} = 0.745$	
						$Nm = 0.15$	

df, degrees of freedom; SS, sum of squares; MS, mean of squares; % Est. Var., estimated variance; *Nm*, inferred gene flow.

bimodal variance (5% quantile 278; 95% quantile 9,491) although largely situated within the Holocene period when considering $t = 3$ years. The posterior distribution of effective sizes was of ancestral (bottlenecked) size $N_{e1} = 914$ and current effective size $N_{ex} = 4,039$ (Supplementary Figure S1). When zooming in on the demographic evolution of the three regions in Vietnam, using a set of all seven possible “origin” scenarios (Supplementary Figure S2), scenario 6 was best supported (50% votes, 0.57 probability) for a phylogeographic scenario where the southern Vietnam populations (estimated $N_{e3} = 2,510$ with 5% quantile = 1291 and 95% quantile = 6,123) have diverged from an ancestral population ($N_{eA} = 2,813$ with 5% quantile = 444 and 95% quantile = 9,057) in the past at $td = 4,414$ (median with 5% quantile = 1,023 and 95% quantile = 9,101), whereas northern Vietnam populations ($N_{e1} = 2,425$ with 5% quantile = 1,021 and 95% quantile = 5,785) diverged most recently at $t_1 = 1,545$ (median with 5% quantile = 445 and 95% quantile = 2,611) from central situated populations ($N_{e2} = 1,578$ with 5% quantile = 564 and 95% quantile = 3,305) (Figure 4B, Supplementary Figure S6).

3.4 Chloroplast genome variants of Southeast Asian *A. marina*

The assemblages averaged 13,316–119,539 reads with a mean depth of reads ranging from 27 to 239 coverage. The aligned plastomes of 150,302-bp length were very similar, and their % of identity ranged from 98.96% to 99.78% for comparisons between three Southeast Asian regions and from 99.83% to 100% between Vietnamese populations. For the considered Southeast Asian *A. marina* populations, we detected 128 mutational changes, namely, 35 transitions, 43 transversions, 9 insertions–deletions, and 41 mononucleotide repeats (Supplementary Table S3). A haplone network incorporated all mutational changes and indicated all stepwise modifications of three clearly distinguishable haplogroups A, B, and C, corresponding to individual trees from Vietnam, Peninsular Malaysia, and the island Leyte in the Philippines, respectively (Figure 5). Within Vietnam, 23 mutations (3 transitions, 4 transversions, 1 indel, and 15 mononucleotide microsatellites) across nine haplotypes could be



detected. The southernmost site (S10, Cà Mau Peninsula) was the most divergent among Vietnam populations and somewhat closer positioned to haplotypes of Peninsular Malaysia.

3.5 Nuclear rRNA cistron variants of *A. marina*

A 5,772-bp nuclear ribosomal cistron was obtained for one sample (from the C7 population) and used as a reference to map every sample, averaging 3,932–23,717 reads with a mean depth of reads ranging from 123 to 713 coverage. The nuclear ribosomal cistron was composed of the 18S small subunit rRNA (1 > 1785, 1785 bp), the internal transcribed spacer region ITS1 (1,786 > 2,018; 233 bp), the 5.8S rRNA subunit (2,019 > 2,181; 163 bp), the internal transcribed spacer region ITS2 (2,182 > 2,403; 222 bp), and the 26S large subunit rRNA (2,404 > 5,772; 3369 bp). This nuclear ribosomal cistron was consistent for *A. marina*, although it contained no mutations for 100% of the covered reads and only non-concerted evolution at 21 nucleotide positions (Supplementary Table S4). These incomplete homogenizations of nucleotide transitions were found in samples from southern Vietnam (six

mutating nucleotide positions), central and northern Vietnam (two mutating nucleotide positions, although none were detected for populations N2 and N3), Malaysia (6), and the Philippines (15), of which one mutating position was shared between Vietnam (N, C, and S regions) and Malaysia, one was shared between southern Vietnam and the Philippines, and three were shared between Malaysia and the Philippines.

4 Discussion

Southern populations were verified for potential hybridization with co-occurring *A. alba*. Few backcrosses of F₂ hybrid individuals and one F₂ individual could be detected, which were removed from all further analyses that were performed on pure *A. marina*. In this study, the genetic diversity, structure, and demographic evolutionary history of *A. marina* populations across Vietnam were assessed using nuclear microsatellite markers and supplemented with complete chloroplast genome and nuclear ribosomal cistron sequences, which altogether reflected a migration history following the coastal shift on the Sunda Shelf. An overall northward directionality of historical migration was

TABLE 4 Comparison of migration models in MIGRATE-n on the directionality of *Avicennia marina* population groups (northern, central, southern region) and testing hypothesis of prevailing northward coastal current direction along the Vietnam coastline. Model outcome of DIVMIGRATE from a relative directional migrate matrix based on G_{ST} and 1000 permutations.

Migration model	Directionality	Connectivity	Outcome		
MIGRATE-n		Connected regions	Bezier log marginal likelihood	Model choice	Model prob
Panmixia	All (full model)	All	-1,035,166.36	4	0
Stepping stone	Bidirectional	N \leftrightarrow C \leftrightarrow S	-882,786.39	3	0
Stepping stone	Unidirectional from north to south	N \rightarrow C \rightarrow S	-836,215.27	2	0
Stepping stone	Unidirectional from south to north	N \leftarrow C \leftarrow S	-810,108.88	1	1
DIVMIGRATE		Connected populations	G_{ST} value (relative)	Sign.	
Stepping stone	Unidirectional and only relevant for northern populations in a northward direction. Significant connectivity was obtained between most northern populations except for N3	N2 \rightarrow N1 N4 \rightarrow N1 N5 \rightarrow N4 N5 \rightarrow N1 N5 \rightarrow N2	0.39 0.26 0.86 1 0.55	* * * * *	

Connected population groups with \leftrightarrow referring to bidirectional and \rightarrow or \leftarrow to unidirectionality. Significant values of G_{ST} between 0.25 and 1 are indicated.

found from southern to northern regions, as well as within the northern region. The southern populations were more diverse and differentiated than those of other regions.

Based on nuclear microsatellites, a demographic model supported an expansion of the species during the Holocene (approximately $t = 4,800$ generations) spanning the whole coastline and with a total effective population size of approximately $N_e = 4,000$. Most populations showed a high inbreeding level and an overall strong differentiation, following an isolation-by-distance model, including an intra-regional subdivision between southern *A. marina* populations. A haplotype network considering all mutational positions of complete chloroplast genomes revealed the presence of either identical or nearly similar maternal propagule source of *A. marina* throughout Vietnam—except for the Cà Mau Peninsula in southern Vietnam—thereby supporting the abovementioned Holocene expansion over a large part of the coastline. Microsatellites, cpDNA, and sequences of the nuclear rRNA cistron confirmed unique alleles and mutations of *A. marina* from Cape Cà Mau on the southern tip of the Mekong delta, whereas a distant relationship of these southern populations with other Southeast Asian populations was shown. A longer-term persistence of *A. marina* along the enlarged shelf zone at the Cà Mau Peninsula can be assumed.

Divergence of central from southern populations was estimated to correspond to the Early Holocene, whereas a further split between central and northern populations would correspond to the Middle Holocene. Additionally, the nuclear rRNA cistron was similar throughout Vietnam except for *A. marina* trees of the Cà Mau Peninsula, confirming a recent common or shared origin of central and northern populations. The low level of rRNA sequence diversity of *A. marina* in the inner sea (Tonkin Gulf) and bordering the shelf of the East Sea may partly be explained by sufficient historical stepping-stone connectivity, currently spread over larger

distances within this oceanic region. We will further discuss encountered aspects of hybridization, diversity, inbreeding, connectivity and migration, the status of diverged populations within a context of coastline features, and perspectives on conservation issues.

4.1 Hybrid detection

Based on the PCoA and genealogical classes at the individual level, only “pure” *A. marina* could be selected for further analysis of the southern individuals and populations. We assume that possible cases of *Avicennia* hybridization in Vietnam (or elsewhere) could be underestimated because the leaf features of those trees that we identified *a posteriori* as F_2 hybrids or backcrosses in our study did resemble *A. marina* morphologically. Such morphological similarity of leaves from genetically intermediate adult trees now can be explained by their genetic identity as a backcross with *A. marina*. This phenomenon of hybridization between two species without obvious morphological expression was also reported for *Avicennia* from the East Malay Peninsula (Triest et al., 2021b).

Hybridization is not uncommon in mangroves. According to Ragavan et al. (2017), the natural hybrids in mangroves are predominantly found in seven genera, namely, *Acrostichum*, *Avicennia*, *Bruguiera*, *Ceriops*, *Lumnitzera*, *Rhizophora*, and *Sonneratia*. It was proposed by Le and Le (2024) that the existence of natural hybridization between *Sonneratia caseolaris* and *S. alba* in southern Vietnam could possibly explain their higher levels of allelic richness and heterozygosity when compared to northern populations void of hybrids. In the case of *Avicennia*, two hybrids—one from Thailand with the parental species of *A. marina* and *Avicennia rumphiana* and another from Brazil with the parental species of *Avicennia germinans* (L.) Stearn and *Avicennia bicolor* Standley—were reported (Huang et al., 2014; Mori et al.,

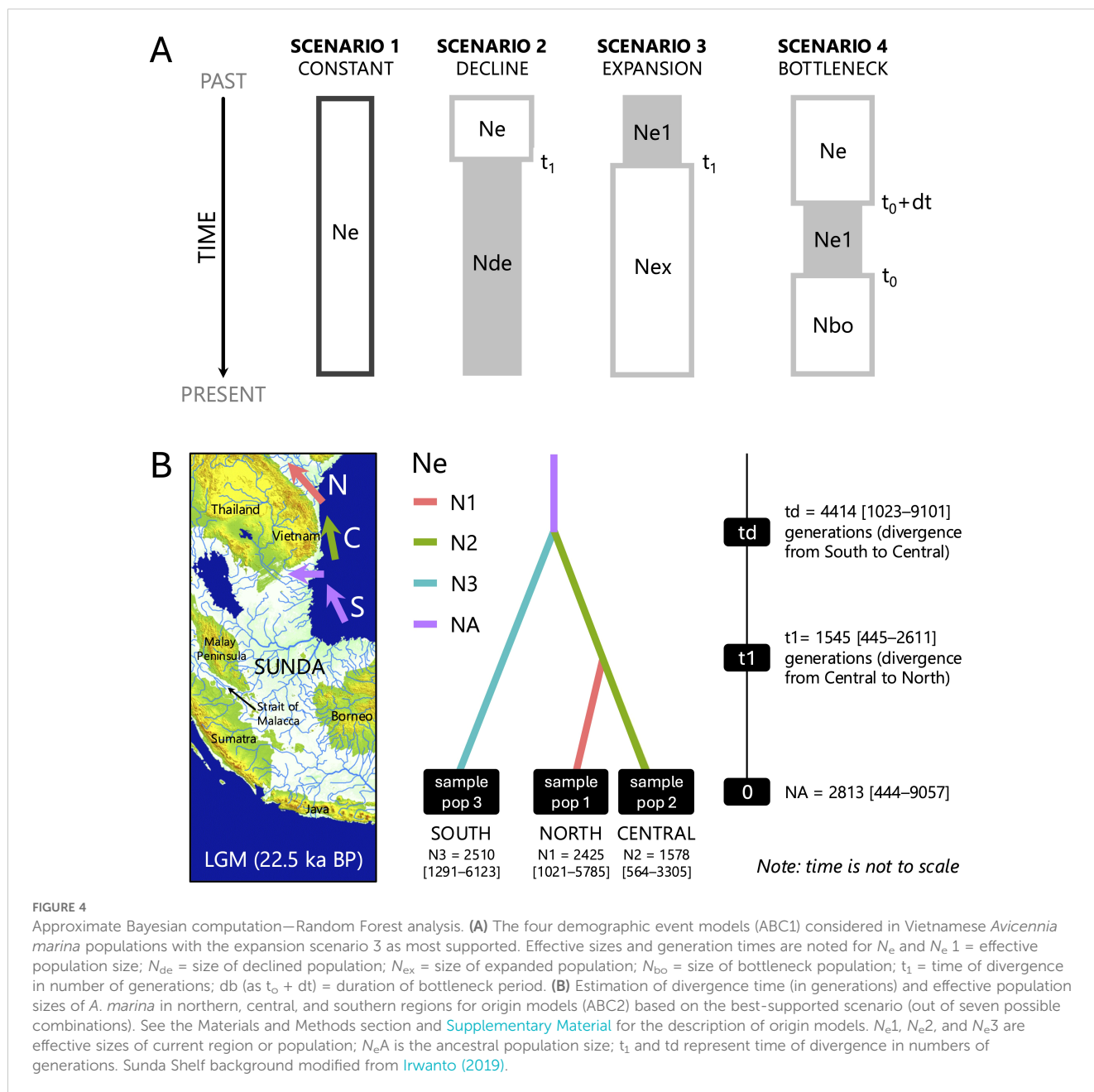


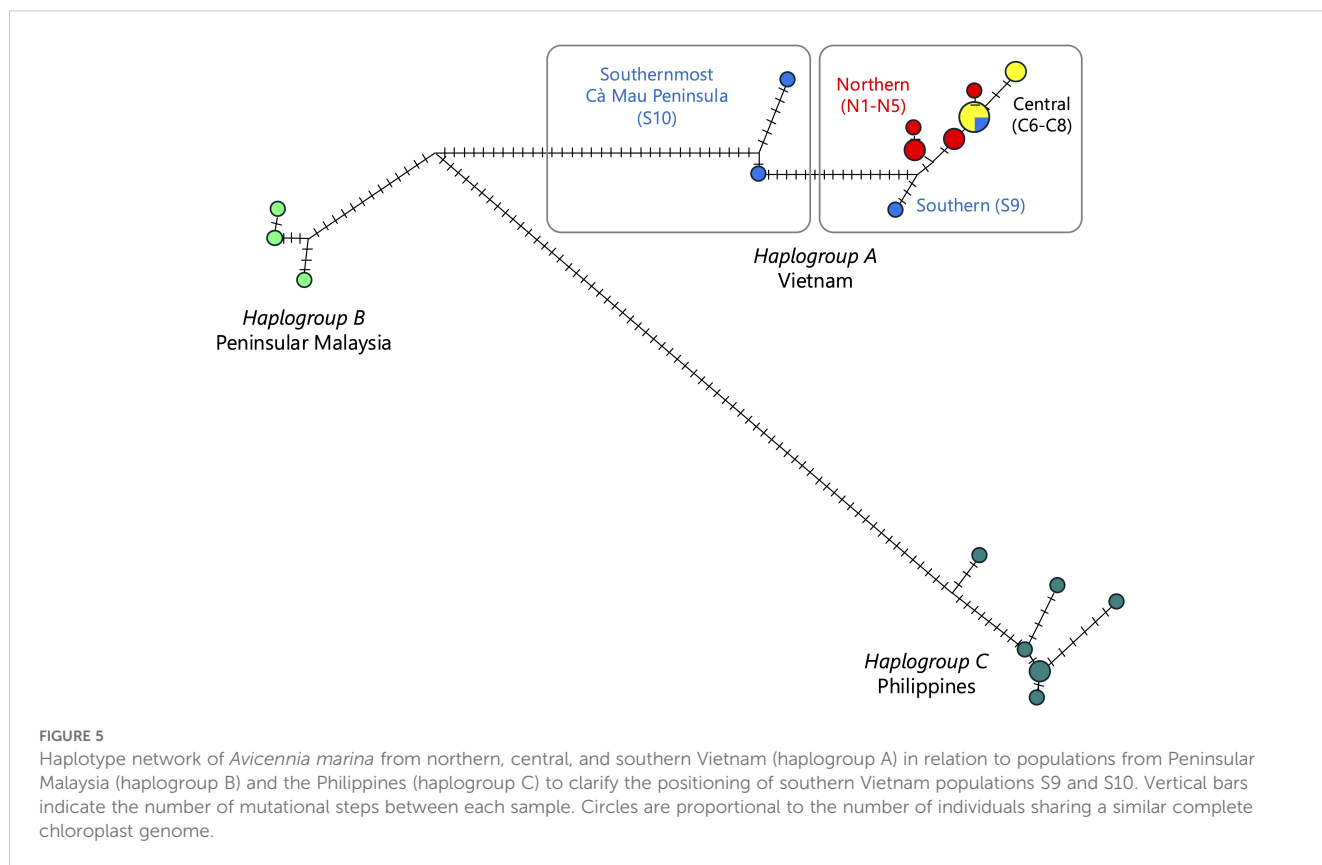
FIGURE 4 Approximate Bayesian computation—Random Forest analysis. **(A)** The four demographic event models (ABC1) considered in Vietnamese *Avicennia marina* populations with the expansion scenario 3 as most supported. Effective sizes and generation times are noted for N_e and N_{e1} = effective population size; N_{de} = size of declined population; N_{ex} = size of expanded population; N_{bo} = size of bottleneck population; t_1 = time of divergence in number of generations; db (as $t_0 + dt$) = duration of bottleneck period. **(B)** Estimation of divergence time (in generations) and effective population sizes of *A. marina* in northern, central, and southern regions for origin models (ABC2) based on the best-supported scenario (out of seven possible combinations). See the Materials and Methods section and [Supplementary Material](#) for the description of origin models. N_{e1} , N_{e2} , and N_{e3} are effective sizes of current region or population; N_{eA} is the ancestral population size; t_1 and t_d represent time of divergence in numbers of generations. Sunda Shelf background modified from [Irwanto \(2019\)](#).

2015b). In a previous study along the east coast of the Malay Peninsula, an introgressive *A. marina* featuring a leaf morphology of *A. marina* and a captured chloroplast of *A. alba* was found (Triest et al., 2021b). Therefore, it is recommended to supplement nuclear DNA markers with chloroplast sequences in regions where several *Avicennia* species co-occur.

4.2 Genetic diversity, structure, and migration directionality along the coast of Vietnam

Allelic richness (A_R) and gene diversity (uH_E) of *A. marina* populations were generally low although informative at both the

population and region levels. *A. marina* populations appeared significantly inbred and subject to recent founder events (i.e., several generations) as could be revealed from bottleneck tests. We commonly observed high and significant inbreeding levels in approximately half of the *A. marina* populations from many regions in Africa and Asia, which therefore may reflect the species' local reproductive biology (Triest, 2008; Triest and Van der Stocken, 2021; Triest et al., 2020, 2021a, b, e). A clear structuring was observed at the region level with substructures at the population level due to overall high levels of genetic differentiation, although structuring was lower between populations of the northern region. Previous studies on *A. marina* of Vietnam also showed a low diversity of alleles, a large differentiation between populations or regions, and significant within-population inbreeding levels based



on five microsatellite loci (Giang et al., 2003), seven loci (Arnaud-Haond et al., 2006), or 15 loci (Do et al., 2019). These basic population genetic features were again confirmed throughout the current study. Elevated levels of inbreeding in *A. marina* sites may be explained by a lack of pollen flow and non-random mating (Arnaud-Haond et al., 2006). However, in turn, high levels of inbreeding within each population may explain a strong differentiation between populations, hence low connectivity.

Despite this overall low level of allelic richness (A_R) and gene diversity (uH_E) of *A. marina* in the study area, MIGRATE-n model tests clearly supported a northward unidirectional stepping-stone migration route from south to central to north, as explained by the allelic variance and thereby supporting to follow a likely history of prevailing northward oceanic currents along a large part of the Vietnamese coastline. At a more detailed level within the northern region, there was an indication of northward migration, which corresponds to the modeling of surface currents based on wind forcing showing a northward direction during summer months in the Gulf of Tonkin (Ding et al., 2013). Wind is non-negligible as a driver in propagule dispersal (Van der Stocken et al., 2015b) to explain the migration directionality obtained from genetic data. However, connectivity patterns of mangrove settlement between estuaries of the same coastline and different habitats thereof are more complicated. Estuarine landscapes are highly diverse and unique in their complexity such that the establishment of *A. marina* propagules is dependent on suitable habitats due to sedimentation patterns of coastal and major river systems, channels or creeks, and sandbar dunes (Triest and Van der

Stocken, 2021). A suite of features can interact with the local distribution of individual genotypes and evoke an inbreeding effect through non-random mating.

A northward migration from a less diverse N5 toward N1 and N2 can be explained by a few additional alleles, differing by only a single mutational step in the latter populations. These minor differences allowed for inferring historical connectivity, as well as identifying their contemporary genetic clusters. Despite their geographical proximity, sites N5 and N4 show lower allelic richness (A_R) and gene (uH_E) diversities at first. This may be explained by their different hydrological situations. The N4 population receives natural flowing water from small branches of the Hong River (in the core zone of Xan Thuy National Parc and near Ba Lat River mouth), whereas N5 receives water from man-made water channels in an area with anthropogenic activities (particularly bivalve farming), thereby being isolated from other mangrove areas by water channels and roads (Jhaveri et al., 2018). Previous research on East African *A. marina* indeed showed that it is important to consider separate transects or patches, even within estuaries (Triest et al., 2020; Triest and Van der Stocken, 2021).

The lowest microsatellite allelic richness and variance were encountered on the northern coast of Vietnam, where the strongest barriers became apparent among a few populations, even at small distances of ca. 30 km (between N3 and neighboring populations). Although the estimated relative migration (here based on the population genetic variable G_{ST}) was largest and unidirectional for northern populations, site N3 appeared the most isolated. Because all northern populations

showed a lack of observed heterozygotes, we hypothesize that an explanation for the lack of connectivity with N3 should come not only from the effect of an inbred situation (since all populations were inbred) but also from a geographical barrier potentially caused by an outflow of the Red (Hong) River where N3 is located and by isolation from northern populations due to the Thai Binh River mouth. Observed high levels of inbreeding may refer to various local processes during most recent generations. Therefore, one should remain critical with information about population genetic structuring in *A. marina* because this can be influenced by local inbreeding events (Arnaud-Haond et al., 2006), in particular, observed at range edges, as evidenced at *A. marina*'s range limit in South Africa (De Ryck et al., 2016). A multi-species approach showed that fragmented mangrove populations, within a distance of a few hundred kilometers along Hainan and the range limit in southern mainland China, were isolated one from another with low levels of contemporary gene flow (Geng et al., 2021). Over even shorter distances within the Gulf of Tonkin, *A. marina* populations already revealed a substructure of several gene pools in northern Vietnam (Do et al., 2019). Similar to our findings, the *S. caseolaris* (L.) Engl. populations of Vietnam showed their lowest level of diversity at its range edge in the northern region and highest in the southern regions, with a central population most related to the northern ones (Le and Le, 2024).

The identical nuclear rRNA cistron and a haplotype network with nearly identical complete chloroplast genomes in the central and northern *A. marina* populations deliver supplementary evidence of a strong relatedness—thus sharing a recent common origin—between these central and northern populations. This agreed with Geng et al. (2021) reporting a low number of haplotypes and low level of polymorphic chloroplast microsatellite loci in *A. marina* from opposite the same Gulf of the Hainan coastal region. We propose that founder events were relatively recent and that most—if not all—populations along the Vietnam coastline originate from the same gene pool as propagule source during the Holocene sea-level rise of the Sunda Plateau. Undoubtedly, the three regions in Vietnam share the same—unknown—maternal propagule source as shown by the haplotype network. There are no documented plantation efforts of *A. marina* using source material between regions that could cause an artificial interregional dispersal (Hung and Stive, 2022).

4.3 Substructure in Southern Peninsula

The southern Vietnam populations were the most diverse for all three considered markers. First, a genetic break between central and southern populations was clearly supported by the AMOVA, STRUCTURE, and BARRIER analyses, whereas allele size differences indicated an evolutionary signal of a longer-lasting divergence with isolation by distance. The R_{ST} was larger than the F_{ST} , which indicates that the microsatellite allele sizes bear an evolutionary signal among the three considered regions, and this was the most pronounced in the south. Second, nuclear microsatellites additionally indicated a clear barrier among southern populations

themselves, in addition to their differentiation from the central Vietnam populations. Although all individuals of S10 appeared admixed in a STRUCTURE outcome (possibly due to uneven sampling), these 13 trees were clearly assigned to their own population in an assignment test. Southern populations S9 and S10 each contained several distinct private alleles at high frequencies (Supplementary Table S1), explaining their genetic clusters and separation in PCoA. These southern populations are at a distance of >600 km, separated by the Mekong delta with an extended peninsula, and thus reflect a different history each, as could be shown from the haplotype network. In a similar manner for microsatellites, the haplotype network showed a substantially larger number of mutational steps in complete chloroplast genomes and especially separated the southernmost Cà Mau Peninsula individuals (S10) from all others. Chloroplast genomes and nuclear rRNA cistron sequences, in addition to the largest fraction of private alleles in microsatellite loci, confirmed the uniqueness of *A. marina* from Cape Cà Mau on the southern tip of the Mekong delta. One haplotype of the southern region population in the Thủy Triều lagoon (S9) was more common and also shared with central populations. S9 is situated at approximately 620 km from the peninsula although only 385 km from central region populations.

However, the barriers to genetic connectivity not only may be attributed to geographical distances but also may come from land masses and different migration histories (Triest, 2008; Hodel et al., 2018; Wee et al., 2020; Triest et al., 2021b) or opposing ocean currents (Mori et al., 2015b; Ngeve et al., 2017). The coastline of Vietnam has particular features to consider such as the enclosed Gulf of Tonkin, a central coastline exposed to northward converging ocean currents, and the southern peninsula with large river delta and sedimentation patterns. The genetic break between the southern and central regions most likely can be explained by regional oceanic currents along the narrowest flooded strip of the Sunda Shelf (i.e., at the eastward bent of the mainland) where the current in summer is northward and separates from the coast between 12°N and 14°N (Shaw and Chao, 1994). For *S. caseolaris* of the northern, central, and southern mangrove regions of Vietnam (Le and Le, 2024), comparable to our study, it was suggested that an intrusion of exotic genetic material (seeds and propagules dispersed from Indonesia, Malaysia, and the Philippines) brought to Vietnam by the southwest monsoon in summer by ocean currents, although with a change in the direction of the current at latitude 12°N, could be considered one of the possible causes of the stronger genetic divergence of the southern populations from those in the central region. Our study also supported such a hypothesis of the effect of oceanic currents diverging. This may explain different historical events of colonization with the unique diversity of the southern populations during the flooding of the Sunda Plateau. Radiocarbon dating of mangroves and shallow marine sediments of the Sunda Shelf (Singapore) indicated stable shorelines and delta initiation at approximately 7,500 BP followed by a stepwise sea-level rise and thus potential coastal dispersal within narrow time intervals (Bird et al., 2007).

Barriers to genetic connectivity may also come from very large rivers (Triest et al., 2018). It is here further hypothesized that the

shallowest zones of the Sunda Shelf with very broad river delta plumes such as the Mekong River may provide a quasi-permanent perpendicular barrier alongside coastal mangrove connectivity. A massive outflow of river water in the upper layers—with freshwater being lighter than saltwater—of the coastal waters, prevents the propagules from directly “crossing” such physical water mass barrier along the main coastline, thereby maintaining the unique diversity of the Cà Mau Peninsula. Other examples of this phenomenon are the wide Brahmaputra River branches in the Sundarbans (Triest et al., 2018), although smaller rivers or delta plumes with a strong seasonal outflow may evoke similar and more local effects (Triest et al., 2020), and regional habitat discontinuity (Binks et al., 2019). It was reported that the interaction between a southwest monsoon and buoyancy-driven flow from the Red (Hong) River, with the highest discharge rates in (late) summer, causes a substantial change in ocean current vector size (namely, an intensification) and direction near the water surface (Ding et al., 2013). It may be further hypothesized that colder river water may negatively impact propagule viability. In the current study, we suggest the potential impact of the Red River on coastal waters (Quartel et al., 2007) to explain a genetic barrier between N3 and other northern Vietnam populations.

4.4 Regional patterns and divergence times

The ABC origin model obtained from microsatellites suggested a more recent expansion of *A. marina* populations along the central and northern coasts of Vietnam when compared to expansion along the southern coasts of Vietnam and the Cà Mau Peninsula. Bottleneck events and founder effects were previously suggested—although not tested or modeled—to have affected *A. marina* populations during Pleistocene glaciations and subsequent transgressions in the South China Sea (Giang et al., 2003; Arnaud-Haond et al., 2006). Our study could confirm an ancestral bottleneck population, followed by a demographic Holocene history of expansion for the species in Vietnam.

The estimated time of expansion event of the Vietnamese population as a whole (ABC analysis considering microsatellites) was estimated at $t_1 = 4,816$ (~14,000–24,000 years when considering $t = 3$ to 5, see Materials and Methods) and their south to central to northern region divergences at $t_d = 4,414$ generations (~13,000–22,000 years) in the Early Holocene (< 6,200 BP) and $t_1 = 1,545$ (~3,000–8,000 years) toward the end of the Early Holocene and the onset of the Middle Holocene (6,200–3,000 BP). Variability in microsatellite allele sizes supported a species origin model that pointed to discrete historical migration events, with southern populations closest to an ancestral bottleneck population. Additionally, the shared but few mutational positions of the nuclear ribosomal cistron show the unique position of *A. marina* in southern Vietnam (S9 and S10) in comparison to other populations of Vietnam. Only one incomplete homogenization of a mutated position in the rRNA cistron could be found in all Vietnam populations, and—either coincided or related—that particular mutation was also shared with a similar nucleotide

transition in Malaysian samples. Incomplete homogenization of the nuclear ribosomal cistron indicates recent ongoing evolutionary processes, as can be expected of a young expansion from a common source. Additionally, one may consider that these more ancestral *Avicennia* genotypes still could recover from a vegetated area that underwent chemical defoliation from dense flight paths of spray missions (Stellman et al., 2003) approximately half a century ago and later on by conversion to aquaculture (Veettil et al., 2019).

A large-scale afforestation program from 1975 to 1980 focused on planting *Rhizophora* in the Cà Mau Province. In more recent afforestation and restoration projects, *Avicennia officinalis* and *A. alba* additionally have been used, along with *Rhizophora* and *Bruguiera* species. However, there is no indication that *A. marina* was actively planted during those reforestation efforts (Hung and Stive, 2022; Van et al., 2015). Mangrove expansion happened, although plantations may not have significantly affected the natural allelic diversity of the limited number of observed and discontinuously collected old-aged *A. marina* trees in S10 because, at the time of collection, planting programs did not comprise this species.

Complete chloroplast genomes and sequences of the nuclear rRNA cistron additionally confirmed unique mutations of *A. marina* from Cape Cà Mau (S10) on the southern tip of the Mekong delta. Its distant relationship with other Southeast Asian populations assumes a longer-term persistence along the enlarged shelf zone at the peninsula, including the mid-Holocene sea-level highstand (4,200 BP). Two different haplotypes along the west coast of the Malay Peninsula showed a phylogeographic relationship with either a northern or a putative southern lineage, thereby assuming two *Avicennia* sources facing each other during the Holocene range shift with a prolonged separation in the Strait of Malacca (Triest et al., 2021b). The difference in genetic structure for several species suggests that the Malay Peninsula acts as a “filter” rather than a strict geographical barrier, depending on the dispersal capacity of mangrove species and ocean-surface current patterns (Wee et al., 2020). Having a lower long-distance dispersal capacity, *Avicennia* spp. are more likely to mainly disperse within their oceanic basin (Maguire et al., 2000b), as supported by our results and thus potentially indicating a correlation between dispersal capacity and genetic admixture following the LGM for *Avicennia* species. However, over several thousands of generations (estimated divergence time t_d ranging from 1,023 to 9,101 generations), our estimation of genetic connectivity among *A. marina* populations along the coast of Vietnam through comparison of migration models supported a unidirectional dispersal route that was congruent with prevailing ocean currents. This further emphasizes the relevance of coastal connectivity to mangrove persistence (Van der Stocken et al., 2019a; b) as well as the importance of apparently discrete estuaries. In a study on the impact of habitat discontinuities on gene flow among 21 *A. marina* populations along the Western Australian coastline, Binks et al. (2019) reported occasional long-distance dispersal up to 100 km, which is comparable to the distance between populations along the Vietnam coastline—namely, within a 147-km stretch for northern populations and a 118-km stretch for central

populations in our study. The present findings also add to the compelling evidence of *Avicennia* species generally following a stepping-stone migration model and add to the emerging evidence of a dominant unidirectional gene flow or migration estimates reported in *A. alba* along the west coast of the Malay Peninsula (Wee et al., 2020), *A. marina* in eastern Africa (Triest et al., 2021e), or Leyte Island in the Philippines (Triest et al., 2021a).

5 Perspectives and conservation issues

We further hypothesize that features of coastal morphology should be considered. The shallowest zones with very broad river delta plumes of the Mekong River may provide a quasi-permanent perpendicular barrier to alongshore coastal mangrove connectivity, thereby causing a regional substructure with genetic unicity of the southernmost Cape Cà Mau population. The ancestral position of this southernmost Vietnam population relative to all other populations along the Vietnamese coastline allows for considering it as a “Sunda remnant”. These potential evolutionary significant units of the southern peninsula, characterized by a divergence of both nuclear and chloroplast markers, merit conservation attention. The high likelihood of historical unidirectional stepping-stone migration between adjacent mangroves and the persistence of sharp genetic breaks, such as encountered for a population, south of the Mekong River delta and for a population close to the Red River delta, both add to the importance of considering coastal connectivity as well as natural coastal barriers. Most populations were genetically differentiated, and therefore, conservation actions should focus on the estuary level. The regional differences between northern, central, and southern populations were highlighted by their private microsatellite alleles and their chloroplast haplotypes and require conservation priorities at the national level.

Vietnam with its extensive coastal stretch over approximately 13° latitude and its position in a biogeographically complex region can be expected to harbor mangrove populations with a history of range expansion as well as genetic differentiation between them. Unlike other mangrove species, *A. marina* does not reach its northern latitudinal range limit in Vietnam, but the species is equally subjected to the range dynamics, possibly exacerbated by climate change and sea level changes. The incentives for mangrove restoration in Vietnam mostly follow concerns over coastal erosion, rehabilitation of abandoned aquaculture ponds, and, more recently, carbon sequestration. Worldwide, mangrove restoration has had a bias toward *Rhizophora* spp., and this equally applies to Vietnam. Nevertheless, *Avicennia* spp. including the wide-ranging and eurytopic *A. marina* are important in mangrove structure and function, which comprises coastal protection. Therefore, the species merits attention in the restoration context. While natural mangrove rehabilitation and recruitment are to be preferred wherever possible (Bosire et al., 2008; Zimmer et al., 2022), plantation will be necessary in many places. Reforestation of mangroves through planting has indeed taken place within the mangrove range along the entire coastline of Vietnam (Hai et al., 2020). Raising *Avicennia* spp. in nurseries is costly and labor-intensive (Hai et al., 2020), yet it is the better method for tree survival, as compared to broadcasting

propagules or transplanting juveniles. The present study shows that the legacy of mangrove expansion in the Sunda Shelf and Vietnam, in particular, left population patterns with clear distinct histories along this extensive coastline, also leaving an imprint of the ecological and coastal geomorphological settings of the establishment. Clear genetic breaks and isolation of certain populations give particular identity to various populations of *A. marina* in Vietnam.

Natural rehabilitation, through recruitment (assuming populations suitable as a pool of propagules for dispersal exist), requires the lifting of barriers for dispersal and establishment, mostly of a hydrological and wave attenuation nature (e.g., Bosire et al., 2008; Nguyen, 2018). When initiating active restoration because natural recruitment cannot take place, *A. marina* can also be a prime target, and hereby the character of the respective regional populations should guide the choice of (nursery) and planting material. We further adhere to the guideline that translocations should mimic wild populations (Neale, 2012) and consider source materials from diverse adult remnants. We also underscore the importance of placing translocations near and in existing populations, at distances that enable effective pollen flow to integrate new or expanding populations into a local network so that levels of inbreeding can be minimized. The isolated Red River branch population merits further follow-up for protection, as well as sparsely distributed *A. marina* adult trees of the Cà Mau Sunda remnant gene pool. However, attention should be paid to the genetic swamping of *A. marina* that may occur with other *Avicennia* species to preserve the intrinsic resilience of this eurytopic pioneer species under changing environmental conditions. Conservation strategies for designing marine parks or conservation areas (cf. Dabalà et al., 2023) must aim to preserve the naturally occurring cohesive forces in the long term for mangroves to continue to play their ecological roles in a changing coastal and marine environment.

Data availability statement

The datasets presented in this study can be found in Dryad Digital Repository <https://doi.org/10.5061/dryad.3r2280gss>. The names of the repository/repositories and accession number(s) can be found in the article/Supplementary Material.

Author contributions

LT: Conceptualization, Data curation, Formal analysis, Funding acquisition, Investigation, Methodology, Resources, Supervision, Visualization, Writing – original draft, Writing – review & editing. PH: Investigation, Resources, Writing – review & editing. LD: Funding acquisition, Investigation, Resources, Writing – review & editing, Visualization. AB-M: Funding acquisition, Investigation, Resources, Writing – review & editing. BD: Data curation, Funding acquisition, Investigation, Methodology, Resources, Writing – review & editing. TS: Data curation, Investigation, Methodology, Writing – review & editing. FD-G: Funding acquisition, Investigation, Writing – review & editing. NK: Investigation, Writing – review & editing. TVDS: Conceptualization,

Investigation, Methodology, Visualization, Writing – original draft, Writing – review & editing.

Funding

The author(s) declare that financial support was received for the research and/or publication of this article. This work was supported by the Vrije Universiteit Brussel (VUB; grant number BAS42), the Flemish Inter-university cooperation (VLIR-IUC) with Hue University, the CNRS through the French National program EC2CO (Ecosphère Continentale et Côtière), and IRP-CNRS France-Vietnam (Tropical Ecology Laboratory).

Acknowledgments

We thank Dao Van Tan from Hanoi National University of Education (Vietnam), Van Tran Thi, Tamara Van Dam, and Nguyen Xuan Tung for the fieldwork assistance.

Conflict of interest

The authors declare that the research was conducted in the absence of any commercial or financial relationships that could be construed as a potential conflict of interest.

Generative AI statement

The author(s) declare that no Generative AI was used in the creation of this manuscript.

Publisher's note

All claims expressed in this article are solely those of the authors and do not necessarily represent those of their affiliated organizations, or those of the publisher, the editors and the reviewers. Any product that may be evaluated in this article, or claim that may be made by its manufacturer, is not guaranteed or endorsed by the publisher.

Supplementary material

The Supplementary Material for this article can be found online at: <https://www.frontiersin.org/articles/10.3389/fmars.2025.1565908/full#supplementary-material>

SUPPLEMENTARY FIGURE 1

Four demographic scenarios for *Avicennia marina* along whole coastline of Vietnam. Ten populations are pooled to consider the species demographic evolution. Model 4 (expansion) was selected. Parameter estimates are given for the divergence time (t_1 generations) of expansion, the effective ancestral bottlenecked population size (N_{e1}) and the effective contemporary expanded population size (N_{ex}); Demographic scenario for *Avicennia marina* along whole coastline of Vietnam. Populations are pooled to consider the species demographic evolution. Model 3 (expansion) was selected. Parameter estimates are given for the divergence time (t_1 generations) of expansion, the effective ancestral bottlenecked population size (N_{e1}) and the effective contemporary total population size after expansion (N_{ex}).

SUPPLEMENTARY FIGURE 2

Seven origin models tested with ABC-RF for selection of the most supported scenario of *Avicennia marina* populations from the northern (N1 in red), central (N2 in green) and southern (N3 in blue) region of Vietnam with their ancestral population (NA in purple).

SUPPLEMENTARY FIGURE 3

Population-based PCoA separating the populations of a central and northern group and separating two southern populations. The 1st axis explained 28% and the 2nd axis 22% of the variation.

SUPPLEMENTARY FIGURE 4

Barplot diagram of STRUCTURE analysis with *Avicennia marina* individuals in ten populations of Vietnam for $K = 2$ to $K = 10$ and graphs of Delta K (peak at $K = 2$ and $K = 7$), $\ln P(K)$ and MedMedK method.

SUPPLEMENTARY FIGURE 5

Relative migration network (DIVMIGRATE) of ten *Avicennia marina* populations from Vietnam, showing significant connectivity among most northern populations (N1-N5, except for N3 located near mouth of Red River – see photo). All other populations are strongly diverged for their microsatellite loci.

SUPPLEMENTARY FIGURE 6

Origin model (selected scenario 6) and parameter estimates for effective sizes of *Avicennia marina* populations from the northern (N1), central (N2) and southern (N3) region of Vietnam and the ancestral population (NA). Parameter estimates are given for the divergence from the southern region (t_1 generations) and divergence from the central region (t_1 generations).

SUPPLEMENTARY TABLE 1

Observed frequency of private alleles (length) in loci for each population and their mean frequency for the northern, central and southern region.

SUPPLEMENTARY TABLE 2

Pairwise population differentiation **A**: F_{ST} values between 10 populations along coastline of Vietnam. F_{ST} values below diagonal. Probability, $P(\text{rand} \geq \text{data})$ based on 999 permutations is shown above diagonal; **B**: R_{ST} values between 10 populations along coastline of Vietnam. R_{ST} values below diagonal. Probability, $P(\text{rand} \geq \text{data})$ based on 999 permutations is shown above diagonal.

SUPPLEMENTARY TABLE 3

Chloroplast DNA with 128 mutational changes, namely 35 transitions (ti), 43 transversions (tv), 9 insertion-deletions (indel) and 41 mononucleotide repeats (μsat) in *Avicennia marina* individuals of ten populations in Vietnam, three in West Malaysian Peninsula and seven in The Philippines.

SUPPLEMENTARY TABLE 4

Incomplete homogenization at 21 nucleotide positions of the nuclear ribosomal RNA cistron (SSrRNA, ITS1, 5.8srRNA, ITS2, LsrRNA) in *Avicennia marina* individuals of ten populations in Vietnam, three in West Malaysian Peninsula and seven in The Philippines. Colors indicate the positions with incomplete homogenizations for each region.

References

- Alongi, D. M. (2002). Present state and future of the world's mangrove forests. *Env. Cons.* 29, 331–349. doi: 10.1017/S0376892902000231
- Al-Qathan, R. N., and Alharbi, S. A. (2020). Spatial structure and genetic variation of a mangrove species (*Avicennia marina* (Forssk.) Vierh.) in the farasan archipelago. *Forests* 11, 1287. doi: 10.3390/f11121287
- Anderson, E. C., and Thompson, E. A. (2002). A model-based method for identifying species hybrids using multilocus genetic data. *Genetics* 160, 1217–1229. doi: 10.1093/genetics/160.3.1217
- Arnaud-Haond, S., Teixeira, S., Massa, S. L., Billot, C., Saenger, P., Coupland, G., et al. (2006). Genetic structure at range edge: low diversity and high inbreeding in Southeast Asian mangrove (*Avicennia marina*) populations. *Mol. Ecol.* 15, 3515–3525. doi: 10.1111/j.1365-294X.2006.02997.x
- Azman, A., Ng, K-K-S., Ng, C.-H., Lee, C.-T., Tnah, L.-H., Zakaria, N.-F., et al. (2020). Low genetic diversity indicating the threatened status of *Rhizophora apiculata* (Rhizophoraceae) in Malaysia: declined evolution meets habitat destruction. *Sci. Rep.* 10, 19112. doi: 10.1038/s41598-020-76092-4
- Banerjee, A., Hui, F., Lin, Y., Hou, Z., Li, W., Shao, H., et al. (2022). Phylogeographic pattern of a cryptoviviparous mangrove, *Aegiceras corniculatum*, in the Indo-West Pacific, provides insights for conservation actions. *Planta* 225. doi: 10.1007/s00425-021-03798-8
- Beerli, P. (2006). Comparison of Bayesian and maximum-likelihood inference of population genetic parameters. *Bioinformatics* 22, 341–345. doi: 10.1093/bioinformatics/bti803
- Beerli, P., and Palczewski, M. (2010). Unified framework to evaluate panmixia and migration direction among multiple sampling locations. *Genetics* 185, 313–326. doi: 10.1534/genetics.109.112532
- Berger, B. A., Han, J., Sessa, E. B., Gardner, A. G., Shepherd, K. A., Ricigliano, V. A., et al. (2017). The unexpected depths of genome-skimming data: A case study examining Goodeniaceae floral symmetry genes. *Appl. Plant Sci.* 5, 1700042. doi: 10.3732/apps.1700042
- Binks, R. M., Byrne, M., McMahon, K., Pitt, G., Murray, K., and Evans, R. D. (2019). Habitat discontinuities from strong barriers to gene flow among mangrove populations, despite the capacity for long-distance dispersal. *Divers. Distrib.* 25, 298–309. doi: 10.1111/ddi.12851
- Bird, M. I., Fifield, L. K., Teh, T. S., Chang, C. H., Shirlaw, N., and Lambeck, K. (2007). An inflection in the rate of early mid-Holocene eustatic sea-level rise: A new sea-level curve from Singapore. *Estuar. Coast. Shelf Sc.* 71, 523–536. doi: 10.1016/j.ecss.2006.07.004
- Bosire, J., Dahdouh-Guebas, F., Walton, M., Crona, B. I., Lewis, R. R. III, Field, C., et al. (2008). Functionality of restored mangroves: a review. *Aquat. Bot.* 89, 251–259. doi: 10.1016/j.aquabot.2008.03.010
- Chapuis, M. P., and Estoup, A. (2007). Microsatellite null alleles and estimation of population differentiation. *Mol. Biol. Evol.* 24, 621–631. doi: 10.1093/molbev/msl191
- Clarke, P. J. (1993). Dispersal of Gray Mangrove (*Avicennia marina*) propagules in Southeastern Australia. *Aquat. Bot.* 43, 195–204. doi: 10.1016/0304-3770(93)90021-N
- Collin, F. D., Durif, G., Raynal, L., Gautier, M., Vitalis, R., Lombaert, E., et al. (2021). Extending Approximate Bayesian Computation with Supervised Machine Learning to infer demographic history from genetic polymorphisms using DIYABC Random Forest. *Mol. Ecol. Resour.* 8, 2598–2613. doi: 10.1111/1755-0998.13413
- Curnick, D. J., Pettorelli, N., Amir, A. A., Balke, T., Barbier, E. B., Crooks, S., et al. (2019). The value of small mangrove patches. *Science* 363, 239. doi: 10.1126/science.aaw0809
- Dabalá, A., Dahdouh-Guebas, F., Dunn, D. C., Everett, J. D., Lovelock, C. E., Hanson, J. O., et al. (2023). Priority areas to protect mangroves and maximise ecosystem services. *Nat. Commun.* 14, 5863. doi: 10.1038/s41467-023-41333-3
- Dahdouh-Guebas, F., Friess, D. A., Lovelock, C. E., Connolly, R. M., Feller, I. C., Rogers, K., et al. (2022). Cross-cutting research themes for future mangrove forest research. *Nat. Plants* 8, 1131–1135. doi: 10.1038/s41477-022-01245-4
- Dahdouh-Guebas, F., Koedam, N., Satyanarayana, B., and Cannicci, S. (2011). Human hydrographical changes interact with propagule predation behaviour in Sri Lankan mangrove forests. *J. Experim. Marine Biol. Ecol.* 399, 188–200. doi: 10.1016/j.jembe.2010.11.012
- De Ryck, D. J. R., Koedam, N., van der Stocken, T., van der Ven, R. M., Adams, J., and Triest, L. (2016). Dispersal limitation of the mangrove *Avicennia marina* at its South African range limit in strong contrast to connectivity in its core East African region. *Mar. Ecol. Prog. Ser.* 545, 123–134. doi: 10.3354/MEPS11581
- Dierckxens, N., Mardulyn, P., and Smits, G. (2017). NOVOPlasty: *de novo* assembly of organelle genomes from whole genome data. *Nucleic Acids Res.* 45, e18. doi: 10.1093/nar/gkw955
- Ding, Y., Chen, C., Beardsley, R. C., Bao, X., Shi, M., Zhang, Y., et al. (2013). Observational and model studies of the circulation in the Gulf of Tonkin, South China Sea. *J. Geophys. Res.: Oceans* 118, 6495–6510. doi: 10.1002/2013JC009455
- Do, B. T. N., Koedam, N., and Triest, L. (2019). *Avicennia marina* maintains genetic structure whereas *Rhizophora stylosa* connects mangroves in a flooded, former inner sea (Vietnam). *Estuar. Coast. Shelf Sc.* 222, 195–204. doi: 10.1016/j.ecss.2019.04.005
- Earl, D. M., and von Holdt, B. M. (2012). STRUCTURE HARVESTER: a website and program for visualizing STRUCTURE output and implementing the Evanno method. *Conserv. Genet. Resour.* 4, 359–361. doi: 10.1007/s12686-011-9548-7
- Evanno, G., Regnaut, S., and Goudet, J. (2005). Detecting the number of clusters of individuals using the software STRUCTURE: a simulation study. *Mol. Ecol.* 14, 2611–2620. doi: 10.1111/j.1365-294X.2005.02553.x
- Friess, D. A., Rogers, K., Lovelock, C. E., Krauss, K. W., Hamilton, S. E., Lee, S. Y., et al. (2019). The state of the world's mangrove forests: past, present, and future. *Annu. Rev. Environ. Resour.* 44, 89–115. doi: 10.1146/annurev-environ-101718-033302
- Friis, G., Smith, E. G., Lovelock, C. E., Ortega, A., Marshall, A., Duarte, C. M., et al. (2024). Rapid diversification of grey mangroves (*Avicennia marina*) driven by geographic isolation and extreme environmental conditions in the Arabian Peninsula. *Mol. Ecol.* 33, e17260. doi: 10.1111/mec.17260
- Geng, Q. F., Lian, C. L., Tao, M., Li, Q., and Hogetsus, T. (2007). Isolation and characterization of 10 new compound microsatellite markers for a mangrove tree species, *Avicennia marina* (Forss.) Vierh. (Avicenniaceae). *Mol. Ecol. Notes* 7, 1208–1210. doi: 10.1111/j.1471-8286.2007.01834.x
- Geng, Q., Wang, Z., Tao, J., Kimura, M. K., Liu, H., Hogetsu, T., et al. (2021). Ocean currents drove genetic structure of seven dominant mangrove species along the coastlines of Southern China. *Front. Genet.* 12. doi: 10.3389/fgene.2021.615911
- Giang, L. H., Hong, P. H., Tuan, M. S., and Harada, K. (2003). Genetic variation of *Avicennia marina* (Forss.) Vierh. (Avicenniaceae) in Vietnam revealed by microsatellite and AFLP markers. *Genes Genet. Syst.* 78, 399–407. doi: 10.1266/ggs.78.399
- Goldberg, L., Lagomasino, D., Thomas, N., and Fatoyinbo, T. (2020). Global declines in human-driven mangrove loss. *Global Change Biol.* 26, 5844–5855. doi: 10.1111/gcb.15275
- Goudet, J. (2001). FSTAT version 2.9.3: a program to estimate and test gene diversities and fixation indices (update from version 1.2, Goudet 1995): a computer program to calculate F-statistic. *J. Hered.* 86, 485–486. doi: 10.1093/oxfordjournals.jhered.a111627
- Guo, W., Banerjee, A. K., Ng, W. L., Guo, W., Banerjee, A. K., Ng, W. L., et al. (2020). Chloroplast DNA phylogeography of the Holly mangrove *Acanthus ilicifolius* in the Indo-West Pacific. *Hydrobiol.* 847, 3591–3608. doi: 10.1007/s10750-020-04372-1
- Guo, W., Banerjee, A. K., Wu, H., Ng, W. L., Feng, H., Qiao, S., et al. (2021). Contrasting phylogeographic patterns in *Lumnitzera* mangroves across the Indo-West Pacific. *Front. Plant Sci.* 12. doi: 10.3389/fpls.2021.637009
- Hai, N. T., Dell, B., Phuong, V. T., and Harper, R. J. (2020). Towards a more robust approach for the restoration of mangroves in Vietnam. *Ann. For. Sci.* 77, 18. doi: 10.1007/s13595-020-0921-0
- Hanebuth, T. J. J., and Statterger, K. (2004). Depositional sequences on a late Pleistocene–Holocene tropical siliciclastic shelf (Sunda Shelf, southeast Asia). *J. Asian Earth Sc.* 23, 113–126. doi: 10.1016/S1367-9120(03)00100-7
- Hanebuth, T., Statterger, K., and Grootes, P. M. (2000). Rapid flooding of the Sunda Shelf: a late-glacial sea-level record. *Science* 288, 1033–1035. doi: 10.1126/science.288.5468.1033
- Hasan, S., Triest, L., Afrose, S., and De Ryck, D. (2018). Migrant pool model of dispersal explains strong connectivity of *Avicennia officinalis* within Sundarban mangrove areas: Effect of fragmentation and replantation. *Estuar. Coast. Shelf Sc.* 214, 38–47. doi: 10.1016/j.ecss.2018.09.007
- Heck, N., Goldberg, L., Andradi-Brown, D. A., Campbell, A., Narayan, S., Ahmadi, G. N., et al. (2024). Global drivers of mangrove loss in protected areas. *Conserv. Biol.* 38, e14293. doi: 10.1111/cobi.14293
- Hermansen, T. D., Roberts, D. G., Toben, M., Minchinton, T. E., and Ayre, D. J. (2015). Small urban stands of the mangrove *Avicennia marina* are genetically diverse but experience elevated inbreeding. *Estuar. Coasts* 38, 1898–1907. doi: 10.1007/s12237-015-9955-1
- Hodel, R. G. J., Knowles, L. L., McDaniel, S. F., Payton, A. C., Dunaway, J. F., Soltis, P. S., et al. (2018). Terrestrial species adapted to sea dispersal: differences in propagule dispersal of two Caribbean mangroves. *Mol. Ecol.* 27, 4612–4626. doi: 10.1111/mec.14894
- Huang, L., Li, X., Huang, V., Shi, S., and Zhou, R. (2014). Molecular evidence for natural hybridization in the mangrove genus *Avicennia*. *Pakistan Jf Bot.* 46, 1577–1584.
- Huang, Y., Tan, F., Su, G., Deng, S., He, H., and Shi, S. (2008). Population genetic structure of three tree species in the mangrove genus *Ceriops* (Rhizophoraceae) from the Indo West Pacific. *Genetica* 133, 47–56. doi: 10.1007/s10709-007-9182-1
- Hung, P. M., and Stive, M. J. F. (2022). Managing mangroves and coastal land cover in the Mekong Delta. *Ocean Coastal Manage.* 219, 10613. doi: 10.1016/j.ocecoaman.2021.106013
- Inomata, N., Wang, W.-R., Changtragoon, S., and Szmídt, A. E. (2009). Levels and patterns of DNA variation in two sympatric mangrove species, *Rhizophora apiculata* and *R. mucronata* from Thailand. *Genes Genet. Syst.* 84, 277–286. doi: 10.1266/ggs.84.277
- Irwanto, D. (2019). *Sundaland: Tracing the cradle of civilizations* (Indonesia Hydro Media), 386. Available online at: <https://archive.org/details/sundaland-tracing-the-cradle-of-civilizations> (Accessed May 3, 2025).

- Jhaveri, N., Nguyen, T. D., and Nguyen, K. D. (2018). Mangrove collaborative management in Vietnam and Asia. Tenure and Global Climate Change (TGCC) project. USAID Global – Technical Report. Available online at: <https://www.researchgate.net/publication/334112798> (Accessed May 3, 2025).
- Katoh, K., and Standley, D. M. (2013). MAFFT Multiple Sequence Alignment Software Version 7: Improvements in performance and usability. *Mol. Biol. Evol.* 30, 772–780. doi: 10.1093/molbev/mst010
- Le, S., and Le, T. V. (2024). Genetic diversity and population structure of natural provenances of *Sonneratia caseolaris* in Vietnam. *J. Genet. Engineer. Biotech.* 22, 100356. doi: 10.1016/j.jgeb.2024.100356
- Li, Y. L., and Liu, J. X. (2018). StructureSelector: A web based software to select and visualize the optimal number of clusters using multiple methods. *Mol. Ecol. Resour.* 18, 176–177. doi: 10.1111/1755-0998.12719
- Li, H., Ma, D., Li, J., Wei, M., Zheng, H., and Zhu, X. (2020). Illumina sequencing of complete chloroplast genome of *Avicennia marina*, a pioneer mangrove species. *Mitochondrial DNA B Resour.* 5, 2131–2132. doi: 10.1080/23802359.2020.1768927
- Li, J., Yang, Y., Chen, Q., Yang, Y., Chen, Q., Fang, L., et al. (2016). Pronounced genetic differentiation and recent secondary contact in the mangrove tree *Lumnitzera racemosa* revealed by population genomic analyses. *Sci. Rep.* 6, 29486. doi: 10.1038/srep29486
- Liao, P. C., Havanond, S., and Huang, S. (2007). Phylogeography of *Ceriops tagal* (Rhizophoraceae) in Southeast Asia: The land barrier of the Malay Peninsula has caused population differentiation between the Indian Ocean and South China Sea. *Cons. Genet.* 8, 89–98. doi: 10.1007/s10592-006-9151-8
- Linder, C. R., Goertzen, L. R., Heuvel, B. V., Francisco-Ortega, J., and Jansen, R. K. (2000). The complete external transcribed spacer of 18S-26S rDNA: amplification and phylogenetic utility at low taxonomic levels in Asteraceae and closely allied families. *Mol. Phylogenet. Evol.* 14, 285–303. doi: 10.1006/mpev.1999.0706
- Lu, W., Zou, Z., Hu, X., and Yang, S. (2022). Genetic diversity and mating system of two mangrove species (*Rhizophora apiculata* and *Avicennia marina*) in a heavily disturbed area of China. *Diversity* 14, 115. doi: 10.3390/d14020115
- Luikart, G., Allendorf, F. W., Cornuet, J.-M., and Sherwin, W. B. (1998). Distortion of allele frequency distributions provides a test for recent population bottlenecks. *J. Hered.* 89, 238–247. doi: 10.1093/jhered/89.3.238
- Maguire, T. L., Edwards, K. J., Saenger, P., and Henry, R. (2000a). Characterisation and analysis of microsatellite loci in a mangrove species, *Avicennia marina* (Forsk.) Vierh. (Avicenniaceae). *Theor. Appl. Genet.* 101, 279–285. doi: 10.1007/s001220051480
- Maguire, T. L., Saenger, P., Baverstock, P., and Henry, R. (2000b). Microsatellite analysis of genetic structure in the mangrove species *Avicennia marina* (Forsk.) Vierh. (Avicenniaceae). *Mol. Ecol.* 9, 1853–1862. doi: 10.1046/j.1365-294x.2000.01089.x
- Malé, P.-J. G., Bardon, L., Besnard, G., Coissac, E., Delsuc, F., Engel, J., et al. (2014). Genome skimming by shotgun sequencing helps resolve the phylogeny of a pantropical tree family. *Mol. Ecol. Res.* 14, 966–975. doi: 10.1111/1755-0998.12246
- Manni, F., Guérard, E., and Heyer, E. (2004). Geographic patterns of (genetic, morphologic, linguistic) variation: How barriers can be detected by using Monmonier's algorithm. *Hum. Biol.* 76, 173190. doi: 10.1353/hub.2004.0034
- Mantiquilla, J. A., Shiao, M.-S., Lu, H.-Y., Sridith, K., Sidiq, S. N. M., Liyanage, W. K., et al. (2022). Deep structured populations of geographically isolated nipa (*Nypa fruticans* Wurmb.) in the Indo-West Pacific revealed using microsatellite markers. *Front. Plant Sci.* 13. doi: 10.3389/fpls.2022.1038998
- Manurung, J., Rojas Andrés, B. M., Barratt, C. D., Schnitzler, J., Jönsson, B. F., Susanti, R., et al. (2023). Deep phylogeographic splits and limited mixing by sea surface currents govern genetic population structure in the mangrove genus *Lumnitzera* (Combretaceae) across the Indonesian Archipelago. *J. Syst. Evol.* 61, 299–314. doi: 10.1111/jse.12923
- Minobe, S., Fukui, S., Saiki, R., Kajita, T., Changtragoon, S., Shukor, N. A. A., et al. (2010). Highly differentiated population structure of a mangrove species, *Bruguiera gymnorhiza* (Rhizophoraceae) revealed by one nuclear *GapCp* and one chloroplast intergenic spacer *trnF-trnL*. *Conserv. Genet.* 11, 301–310. doi: 10.1007/s10592-009-9806-3
- Mix, A. L., Bard, E., and Schneider, R. (2001). Environmental processes of the ice age: land, oceans, glaciers (EPILOG). *Quat. Sci. Rev.* 20, 627–657. doi: 10.1016/S0277-3791(00)00145-1
- Mori, G. M., Zucchi, M. I., Sampaio, I., and Souza, A. P. (2015a). Species distribution and introgressive hybridization of two *Avicennia* species from the Western Hemisphere unveiled by phylogeographic patterns. *BMC Evol. Biol.* 15, 1–15. doi: 10.1186/s12862-015-0343-z
- Mori, G. M., Zucchi, M. I., and Souza, A. P. (2015b). Multiple-geographic-scale genetic structure of two mangrove tree species: the roles of mating system, hybridization, limited dispersal and extrinsic factors. *PLoS One* 10, e0118710. doi: 10.1371/journal.pone.0118710
- Müller, K. (2006). Incorporating information from length-mutational events into phylogenetic analysis. *Mol. Phylogenet. Evol.* 38, 667–676. doi: 10.1016/j.ympev.2005.07.011
- Nathan, R., Schurr, F. M., Spiegel, O., Steinitz, O., Trakhtenbrot, A., and Tsoar, A. (2008). Mechanisms of long-distance seed dispersal. *Trends Ecol. Evol.* 23, 638–647. doi: 10.1016/j.tree.2008.08.003
- Neale, J. R. (2012). “Genetic considerations in rare plant reintroduction: practical applications (or How are we doing?).” in *Plant reintroduction in a changing climate* (Island Press/Center for Resource Economics, Washington, DC), 71–88.
- Ngeve, M., van der Stocken, T., Menemenlis, D., Koedam, N., and Triest, L. (2016). Contrasting effects of historical sea level rise and contemporary ocean currents on regional gene flow of *Rhizophora racemosa* in Eastern Atlantic mangroves. *PLoS One* 11, e0150950. doi: 10.1371/journal.pone.0150950
- Ngeve, M., van der Stocken, T., Menemenlis, D., Koedam, N., and Triest, L. (2017). Hidden founders? Strong bottlenecks and fine-scale genetic structure in mangrove populations of the Cameroon Estuary complex. *Hydrobiologia* 803, 189–207. doi: 10.1007/s10750-017-3369-y
- Nguyen, T. P. (2018). *Melaleuca* entrapping microsites as a nature based solution to coastal erosion: A pilot study in Kien Giang, Vietnam. *Ocean Coast. Manage.* 155, 98–103. doi: 10.1016/j.ocecoaman.2018.02.005
- Peakall, R., and Smouse, P. E. (2012). GenAlEx 6.5: genetic analysis in Excel. Population genetic software for teaching and research – an update. *Bioinformatics* 28, 2537–2539. doi: 10.1111/j.1471-8286.2005.01155.x
- Piry, S., Luikart, G., and Cornuet, J. M. (1999). Computer note. BOTTLENECK: a computer program for detecting recent reductions in the effective size using allele frequency data. *J. Hered.* 90, 502–503. doi: 10.1093/jhered/90.4.502
- Pritchard, J. K., Stephens, M., and Donnelly, P. S. (2000). Inference of population structure using multilocus genotype data. *Genetics* 155, 945–959. doi: 10.1111/j.1471-8286.2007.01758.x
- Puechmaile, S. J. (2016). The program STRUCTURE does not reliably recover the correct population structure when sampling is uneven: subsampling and new estimators alleviate the problem. *Mol. Ecol. Res.* 16, 608–627. doi: 10.1111/1755-0998.12512
- Quartel, S., Kroon, A., Augustinus, P. G. E. F., Van Santen, P., and Tri, N. H. (2007). Wave attenuation in coastal mangroves in the Red River Delta, Vietnam. *J. Asian Earth Sci.* 29, 576–584. doi: 10.1016/j.jseas.2006.05.008
- Rabinowitz, D. (1978). Dispersal properties of mangrove propagules. *Biotropica* 10, 47–57. doi: 10.2307/2388105
- Ragavan, P., Zhou, R., Ng, W. L., Rana, T. S., Mageswaran, T., Mohan, P. M., et al. (2017). Natural hybridization in mangroves – an overview. *Bot. J. Linn. Soc.* 185, 208–224. doi: 10.1093/botlinnean/box053
- Ruang-areerate, P., Naktang, C., Kongkachana, W., Sangsarakru, D., Narong, N., Maknual, C., et al. (2022). Assessment of the genetic diversity and population structure of *Rhizophora apiculata* Blume (Rhizophoraceae) in Thailand. *Biology* 11, 1449. doi: 10.3390/biology11101449
- Sathiamurthy, E., and Voris, K. H. (2006). Maps of Holocene sea level transgression and submerged lakes on the Sunda Shelf. *Natural History J. Chulalongkorn Univ.* 2, 1–44.
- Schwarzbach, A. E., and McDade, L. A. (2002). Phylogenetic relationships of the mangrove family Avicenniaceae based on chloroplast and nuclear ribosomal DNA sequences. *Syst. Bot.* 27, 84–98. doi: 10.1043/0363-6445-27.1.84
- Shaw, P. T., and Chao, S. Y. (1994). Surface circulation in the South China Sea. Deep sea research part I. *Oceanographic Res. Papers* 41, 1663–1683. doi: 10.1016/0967-0637(94)90067-1
- Stankiewicz, K. H., Vasquez Kuntz, K. L., Coral Microsatellite Group, and Baums, I. B. (2022). The impact of estimator choice: Disagreement in clustering solutions across K estimators for Bayesian analysis of population genetic structure across a wide range of empirical data sets. *Mol. Ecol. Resour.* 22, 1135–1148. doi: 10.1111/1755-0998.13522
- Stellman, J. M., Stellman, S. D., Christian, R., Weber, T., and Tomasallo, C. (2003). The extent and patterns of usage of Agent Orange and other herbicides in Vietnam. *Nature* 422, 682–687. doi: 10.1038/nature01537
- Straub, S. C. K., Parks, M., Weitemier, K., Fishbein, M., Cronn, R. C., and Liston, A. (2012). Navigating the tip of the genomic iceberg: Next-generation sequencing for plant systematics. *Am. J. Bot.* 99, 349–364. doi: 10.3732/ajb.1100335
- Stuart, S. A., Choat, B., Martin, K. C., Holbrook, N. M., and Ball, M. C. (2007). The role of freezing in setting the latitudinal limits of mangrove forests. *New Phytol.* 173, 576–583. doi: 10.1111/j.1469-8137.2006.01938.x
- Su, G. H., Huang, Y. L., Tan, F. X., Ni, X. W., Tang, T., and Shi, S. H. (2006). Genetic variation in *Lumnitzera racemosa*, a mangrove species from the Indo-West Pacific. *Aquat. Bot.* 84, 341–346. doi: 10.1016/j.aquabot.2006.01.001
- Su, G., Huang, Y., Tan, F., Ni, X., Tang, T., and Shi, S. (2007). Conservation genetics of *Lumnitzera littorea* (Combretaceae), an endangered mangrove, from the Indo-West Pacific. *Marine Biol.* 150, 321–328. doi: 10.1007/s00227-006-0357-6
- Sundqvist, L., Keenan, K., Zackrisson, M., Prodöhl, P., and Kleinhans, D. (2016). Directional genetic differentiation and relative migration. *Ecol. Evol.* 6, 3461–3475. doi: 10.1002/ece3.2016.6.issue-11
- Teixeira, S., Arnaud-Haond, S., Duarte, M., and Serrão, E. (2003). Polymorphic microsatellite DNA markers in the mangrove tree *Avicennia alba*. *Mol. Ecol. Notes* 3, 544–546. doi: 10.1046/j.1471-8286.2003.00505.x
- Urashi, C., Teshima, K. M., Minobe, S., Koizumi, O., and Inomata, N. (2013). Inferences of evolutionary history of a widely distributed mangrove species, *Bruguiera gymnorhiza*, in the Indo-West Pacific region. *Ecol. Evol.* 3, 2251–2261. doi: 10.1002/ece3.624

- The Galaxy Community (2022). The Galaxy platform for accessible, reproducible and collaborative biomedical analyses: 2022 update. *Nucleic Acids Res.* 50, W345–W351. doi: 10.1093/nar/gkac247
- Thomas, M., Nakajima, Y., and Mitarai, S. (2022). Extremely stochastic connectivity of island mangroves. *Front. Mar. Sci.* 9. doi: 10.3389/fmars.2022.827590
- Tomizawa, Y., Tsuda, Y., Saleh, M. N., Wee, A. K. S., Takayama, K., Yamamoto, T., et al. (2017). Genetic Structure and Population Demographic History of a Widespread Mangrove Plant *Xylocarpus granatum* J. Koenig across the Indo-West Pacific Region. *Forests* 8, 480. doi: 10.3390/f8120480
- Triest, L. (2008). Molecular ecology and biogeography of mangrove trees towards conceptual insights on gene flow and barriers: A review. *Aquat. Bot.* 89, 138–154. doi: 10.1016/j.aquabot.2007.12.013
- Triest, L., Del Socorro, A., Gado, V. J., Mazo, A. M., and Sierens, T. (2021a). *Avicennia* genetic diversity and fine-scaled structure influenced by coastal proximity of mangrove fragments. *Front. Mar. Sci.* 8. doi: 10.3389/fmars.2021.643982
- Triest, L., Hasan, S., Mitro, P., De Ryck, D., and van der Stocken, T. (2018). Geographical distance and large rivers shape genetic structure of *Avicennia officinalis* in the highly dynamic Sundarbans mangrove forest and Ganges Delta region. *Estuaries Coast.* 41, 908–920. doi: 10.1007/s12237-017-0309-z
- Triest, L., Satyanarayana, B., Delange, O., Sarker, K. K., Sierens, T., and Dahdouh-Guebas, F. (2021b). Barrier to gene flow of grey mangrove *Avicennia marina* populations in Peninsular Malaysia as revealed from nuclear microsatellites and chloroplast haplotypes. *Front. Conserv. Sc.* 2. doi: 10.3389/fcsc.2021.727819
- Triest, L., Sierens, T., and van der Stocken, T. (2021c). Complete chloroplast genome variants reveal discrete long-distance dispersal routes of *Rhizophora* in the Western Indian Ocean. *Front. Conserv. Sc.* 2. doi: 10.3389/fcsc.2021.726676
- Triest, L., and Van der Stocken, T. (2021). Coastal landform constrains dispersal in mangroves. *Front. Mar. Sci. section Marine Ecosystem Ecol.* 8. doi: 10.3389/fmars.2021.617855
- Triest, L., van der Stocken, T., Akinyi, A. A., Sierens, T., Kairo, J., and Koedam, N. (2020). Channel network structure determines genetic connectivity of landward-seaward *Avicennia marina* populations in a tropical bay. *Ecol. Evol.* 10, 12059–12075. doi: 10.1002/ece3.6829
- Triest, L., van der Stocken, T., De Ryck, D., Kochzius, M., Lorent, S., Ngeve, M., et al. (2021d). Expansion of the mangrove species *Rhizophora mucronata* in the Western Indian Ocean launched contrasting genetic patterns. *Sci. Rep.* 11, 4987. doi: 10.1038/s41598-021-84304-8
- Triest, L., van der Stocken, T., Sierens, T., Deus, E. K., Mangora, M. M., and Koedam, N. (2021e). Connectivity of *Avicennia marina* populations within a proposed marine transboundary conservation area between Kenya and Tanzania. *Biol. Cons.* 256, 109040. doi: 10.1016/j.biocon.2021.109040
- Van, T. T., Wilson, N., Thanh-Tung, H., Quisthoudt, K., Quang-Minh, V., Xuan-Tuan, L., et al. (2015). Changes in mangrove vegetation area and character in a war and land use change affected region of Vietnam (Mui Ca Mau) over six decades. *Acta Oecologica* 63, 71–81. doi: 10.1016/j.actao.2014.11.007
- Van der Stocken, T., Carroll, D., Menemenlis, D., Simard, M., and Koedam, N. (2019b). Global-scale dispersal and connectivity in mangroves. *Proc. Natl. Acad. Sci. U.S.A.* 116, 915–922. doi: 10.1073/pnas.1812470116
- Van der Stocken, T., De Ryck, D. J. R., Vanschoenwinkel, B., Deboelpaep, E., Bouma, T. J., Dahdouh-Guebas, F., et al. (2015a). Impact of landscape structure on propagule dispersal in mangrove forests. *Mar. Ecol. Prog. Ser.* 524, 95–106. doi: 10.3354/meps11206
- Van der Stocken, T., Vanschoenwinkel, B., De Ryck, D. J. R., Bouma, T. J., Dahdouh-Guebas, F., and Koedam, N. (2015b). Interaction between water and wind as a driver of passive dispersal in mangroves. *PLoS One* 10, e0121593. doi: 10.1371/journal.pone.0121593
- Van der Stocken, T., Wee, A. K. S., De Ryck, D. J. R., Vanschoenwinkel, B., Friess, D. A., and Dahdouh-Guebas, F. (2019a). A general framework for propagule dispersal in mangroves. *Biol. Rev.* 94, 1547–1575. doi: 10.1111/brv.12514
- Van Oosterhout, C., Hutchinson, W. F., Wills, D. P. M., and Shipley, P. (2004). MICRO-CHECKER: Software for identifying and correcting genotyping errors in microsatellite data. *Mol. Ecol. Notes* 4, 535–538. doi: 10.1111/j.1471-8286.2004.00684.x
- Veettil, B. K., Ward, R. D., Quang, N. X., Trang, N. T. T., and Giang, T. H. (2019). Mangroves of Vietnam: Historical development, current state of research and future threats. *Estuar. Coast. Shelf Sc.* 218, 212–236. doi: 10.1016/j.ecss.2018.12.02
- Wee, A. K. S., Low, S. Y., and Webb, E. L. (2015). Pollen limitation affects reproductive outcome in the bird-pollinated mangrove *Bruguiera gymnorrhiza* (Lam.) in a highly urbanized environment. *Aquat. Bot.* 120, 240–243. doi: 10.1016/j.aquabot.2014.09.001
- Wee, A. K. S., Noreen, A. M. E., Ono, J., Takayama, K., Kumar, P. P., Tan, H. T. W., et al. (2020). Genetic structures across a biogeographical barrier reflect dispersal potential of four Southeast Asian mangrove plant species. *J. Biogr.* 47, 1258–1271. doi: 10.1111/jbi.1381
- Wee, A. K. S., Takayama, K., Asakawa, T., Thompson, B., Onrizal, O., Sungkaew, S., et al. (2014). Oceanic currents, not land masses, maintain the genetic structure of the mangrove *Rhizophora mucronata* Lam. (Rhizophoraceae) in Southeast Asia. *J. Biogeogr.* 41, 954–964. doi: 10.1111/jbi.12263
- Wee, A. K. S., Teo, J. X. H., Chua, J. L., Takayama, K., Asakawa, T., Meenakshisundaram, S. H., et al. (2017). Vicariance and oceanic barriers drive contemporary genetic structure of widespread mangrove species *Sonneratia alba* J. Sm in the Indo-West Pacific. *Forests* 8, 483. doi: 10.3390/f8120483
- Yahya, A. F., Hyun, J. O., Lee, J. H., Kim, Y. Y., Lee, K. M., Hong, K. N., et al. (2014). Genetic variation and population structure of *Rhizophora apiculata* (Rhizophoraceae) in the greater Sunda Islands, Indonesia using microsatellite markers. *J. Plant Res.* 127, 287–297. doi: 10.1007/s10265-013-0613-z
- Yan, Y. B., Duke, N. C., and Sun, M. (2016). Comparative analysis of the pattern of population genetic diversity in three Indo-West Pacific *Rhizophora* mangrove species. *Front. Plant Sci.* 7. doi: 10.3389/fpls.2016.01434
- Yang, Y., Li, J., Yang, S., Li, X., Fang, L. U., Zhong, C., et al. (2017). Effects of Pleistocene sea-level fluctuations on mangrove population dynamics: a lesson from *Sonneratia alba*. *BMC Evol. Biol.* 17, 22. doi: 10.1186/s12862-016-0849-z
- Zimmer, M., Ajonina, G. N., Amir, A. A., Cragg, S. M., Crooks, S., Dahdouh-Guebas, F., et al. (2022). When nature needs a helping hand: Different levels of human intervention for mangrove (re-) establishment. *Front. For. Glob. Change.* 5. doi: 10.3389/ffgc.2022.784322